

HOM Damping in a TESLA Cavity Model using a Rectangular Waveguide.

A.Blednykh, V.Kaljuzhny, D.Kostin.M.Lalayan, A.Lyapin, O.Milovanov,
A.Ponomarenko, N.Sobenin, A.Sulimov, D.Trubin, A.Zavadtzev
Moscow State Engineering Physics Institute MEPHI (Technical University)
Kashirskoe sh. 31, 115409, Moscow, Russia

M.Dohlus

Deutsches Elektronen-Synchrotron DESY
Notkestr. 85, 22607 Hamburg, Germany.

HOM Damping in a TESLA Cavity Model using a Rectangular Waveguide.

A.Blednykh, V.Kaljuzhny, D.Kostin.M.Lalayan, A.Lyapin, O.Milovanov,
A.Ponomarenko, N.Sobenin, A.Sulimov, D.Trubin, A.Zavadtzev
Moscow State Engineering Physics Institute MEPhI (Technical University)
Kashirskoe sh. 31, 115409, Moscow, Russia

M.Dohlus

Deutsches Elektronen-Synchrotron DESY
Notkestr. 85, 22607 Hamburg, Germany.

Abstract

Some modifications of a Rectangular Waveguide HOM Couplers for TESLA superstructure have been investigated. These RWG HOM couplers were installed between the cavities of the superstructure and also at the both ends of this one. We investigated a RWG HOM coupler attached to the beam pipe through the slots orientated along beam pipe axis (longitudinal slot), perpendicular to it (azimuthal slots) and at some angle to this axis. For damping dipole modes of both polarization two rectangular waveguide in every design were used. This work presents the results of calculations and radiofrequency measurements at two copper cavities of superstructure with a scaled-up model at 3 GHz at room temperature. The advantages of HOM coupler with longitudinal slots for damping dipole modes and compact of HOM coupler with slots at 60° to the axis were shown. Arrangement of HOM coupler in cryostat and heating due to HOM losses are presented. Calculation and design of the feeding rectangular waveguide coupler for superstructure are presented too.

1.Introduction.

We have chosen for our mock-up of superstructure the operational frequency 2.981 GHz. instead of 1.3 GHz to reduce its dimensions. This value of frequency was obtained comparing the dimensions of Rectangular WaveGuides (RWG): the wide side of waveguides was 72mm and 165.1mm correspondingly and therefore scaling $K_{sc1}=2.293$. Also all dimensions of cells were decreased in 2.293 times as compared with TESLA dimensions [1], except one end's cell. Its iris's diameter were 49.70 mm (114mm at 1.3GHz) and 34.04 mm (78mm at 1.3GHz). The diameter of all other iris is 30.54mm (70mm at 1.3GHz). It was manufactured two subcavities, each of them consists seven cells.

We included in report the results of calculation and experimental investigation at fundamental and high order modes for our mock-up, obtained by using MAFIA, SUPERFISH and URMEL codes. Smoothing of the electric field in cavity cells was fulfilled by the method of tuning the cell cavity frequency, using the experimentally found data of electric field distribution on the cavity axis.

We considered two variants of set-up consisting of Feeding Mode (FM) coupler and High Order Mode (HOM) couplers. Originally we examined variant with FM coupler between subcavities and HOM coupler of three RWGs, connected with azimuthal slots with beam pipe. Such device has appeared inefficient for dipole modes damping. Instead of it was offered and investigated a device consisting from two RWs with orientation of slots along an beam pipe axis. The device has appeared is preferable for dipole modes damping. Its disadvantage is some difficulty connected to a insufficient place for an arrangement of RW between two subcavities, as the size by a wide wall of RW is commensurable with beam pipe length. Such devices undoubtedly may be established on the ends of superstructure. The more suitable device for HOM damping between the subcavities is the device with an arrangement of the coupling slot under a some angle to an axis of beam pipe. With the purpose of stooping of operation mode penetration through this device is used the rejector filter. During performance of work it was offered also to transfer of FM coupler from middle between subcavities to a beginning of superstructure.

The results of calculations and experimental researches for all three HOM couplers in the wide frequency band are given in the report. We defined in each case an external quality factor Q_{ext} on the basis of Q-factor measurements without and with HOM dampers. The measurements were carried out in case of use two tuned at operation frequency subcavities with beam pipe between them, and also with two halfcells instead of subcavities. In last case it was done the calculations by HFSS program.

In the report also some variants of arrangement in the cryostat of the considered HOM coupler are given.

2. Tuning of the subcavities.

The dimensions of end cells in every subcavity are different from the middle cell dimensions, because we must obtain the same value of the electric field on the cavity axis (smoothing electric field). We have chosen the iris diameter of the subcavity end cell, connected with waveguide coupler, equal 34.00 mm to obtain the necessary value of external Q-factor. The iris diameter of another cell end was 49.70 mm.

Firstly we have tune the cells of the subcavities at the π mode at operational frequency. The frequency of every cell was tuned at 2981MHz with accuracy ± 0.5 MHz.

Using the URMEL code we have calculated the dispersion characteristics of operational mode and HOM. Calculations were done with resonator's mock-ups, consisting different identical cells and whole or half cells at the ends of mock-up. We used different boundary conditions-electric and magnetic walls. Calculated dispersion characteristics are presented at Fig.1.

The second stage of the investigations was connected with smoothing of the electric field on the axis of the subcavities. This work was carried out firstly with using of SUPERFISH code and then the end's cells of subcavities were tuning during the experimental investigations. The calculations were done for structure, using the setup, consisting of three and half cells and beam pipe with length 100mm at the end's cell. During the calculations were used the electric walls at the ends of this setup. The electric field distribution along the axis for the half structure how with the iris 49.70mm and also 34.04 mm for the end cells were calculated separately. The influence dimension R_0 of the end cell with iris 49.70 mm at the distribution of the electric field are presented at Fig.2a,b. How one can see from these pictures the field in the last cell and the frequency of setup are increasing with decreasing of the dimension R_0 . At the same time the field in other cell is decreasing. The optimal variant with smoothing of electric field was obtained for the case with R_0 equal 45.802mm. The analogic data for another haft of structure (with iris 34.04 mm for the end cell) are presented at Fig.3 a,b. Here we see again that with decreasing of dimension R_0 the electric field in the end's cell increasing and decreasing in other cells. The optimal variant was obtained with the dimension R_0 equal 45.02mm.

F, MHz

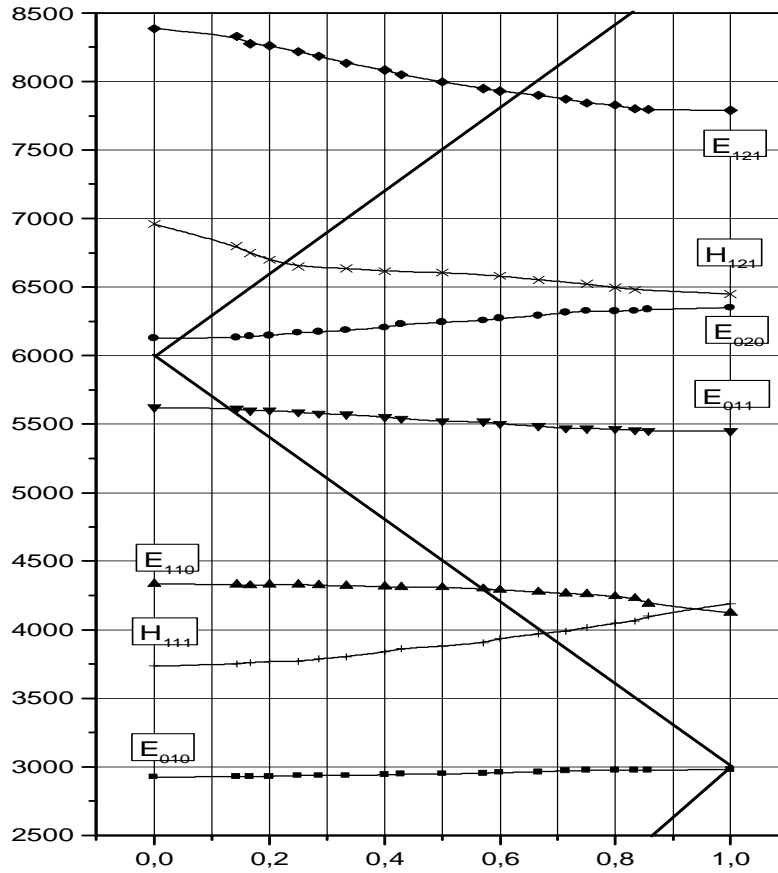


Fig.1. Dispersion characteristics of operational mode and HOM for TESLA cavity model

We have got for these two half subcavities the following values of irregular electric field in the neighboring cells and frequencies of the operation mode: 4% at the frequency 2985 MHz for half cavity with end cell with iris diameter 49.70 mm (we will call this cell as end cell # 2) and 5% at the frequency 2986 MHz for half cavity with end cell with iris diameter 34.04 mm (we will call this cell as end cell # 1 and it will be attached to rectangular waveguide coupler). We decided to leave these values of frequencies, because we will have in our setup rectangular waveguide coupler and some installations for HOM damping additionally and therefore we will tune our setup at frequency 2981 MHz.

Fig.4 shows the electric field distribution in two subcavities, connect by $\lambda/2$ beam pipe in circular waveguide. Obviously, this method of smoothing of electric field, using two setups, each of them consists half subcavity, has given rather good result. The dimensions of middle cells and both end cells, which were got after smoothing of field at operation frequency, are pointed out in the Table 1. Here R_0 is equator radius, R is radius of circular arc, L is length of half-cell, r_i is iris radius, a -is horizontal half axis, b -is vertical half axis. The data in line N 3 and N5 fit the dimensions of half of end cells. The data in line N2 and N4 are the data of the second half of these end cells.

Table 1. The dimensions of tuned subcavity cells.

N	R ₀ ,mm	R,mm	L,mm	r _i ,mm	a,mm	b,mm
1	45.035	18.33	25.16	15.27	5.24	8.29
2	45.802	18.10	25.16	15.27	5.24	5.24
3	45.802	18.10	24.44	24.85	5.29	6.46
4	45.01	18.33	25.16	15.27	5.24	5.24
5	45.01	18.33	24.87	17.02	4.36	5.90

These calculations were used during the experimental tuning of two subcavities at operation frequency 2981 MHz with smoothing of electric field on the axis of subcavity. Each subcavity was tuned at the operation mode frequency before brazing using the technique, described in Appendix 1. Because these subcavities must be attached one with another through beam pipe with length $\lambda/2$, we tuned every subcavity with beam pipe length $\lambda/4$ and short-circuited at one end and long beam pipe at another end. How one can see from Fig. A-1, irregular electric field in the neighboring cells and frequencies for two subcavities are 2.53% and frequency 2982.04 MHz for one subcavity and 2.21% and frequency 2982.06 MHz for the second subcavity.

At Fig.5 one can see the final result for two subcavities, obtained after tuning separately two half-cell of the subcavity with different end's cell.

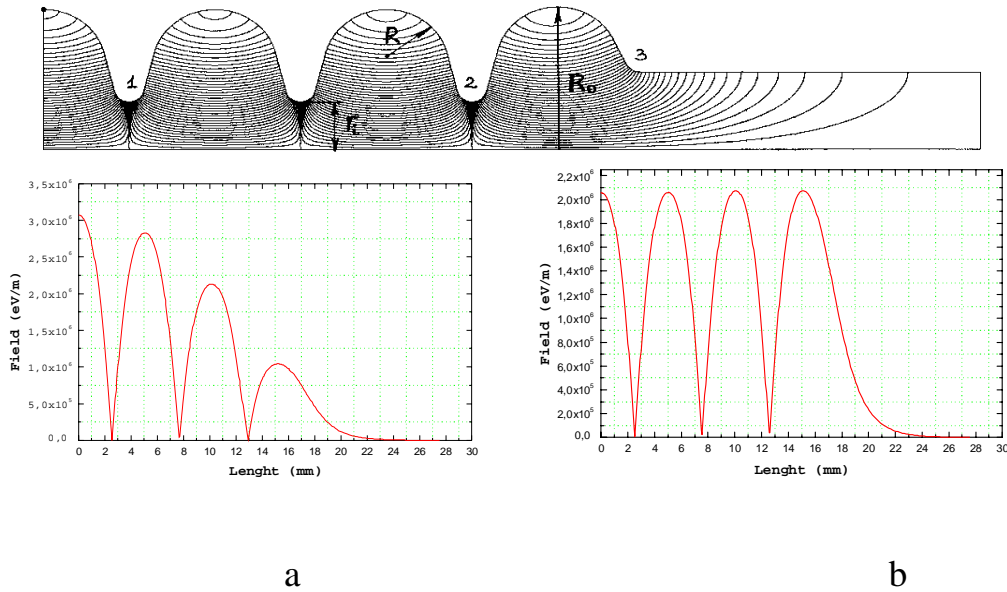


Fig.2. Electric field distribution on the axis of the half subcavity with the large beam pipe (calculated data)

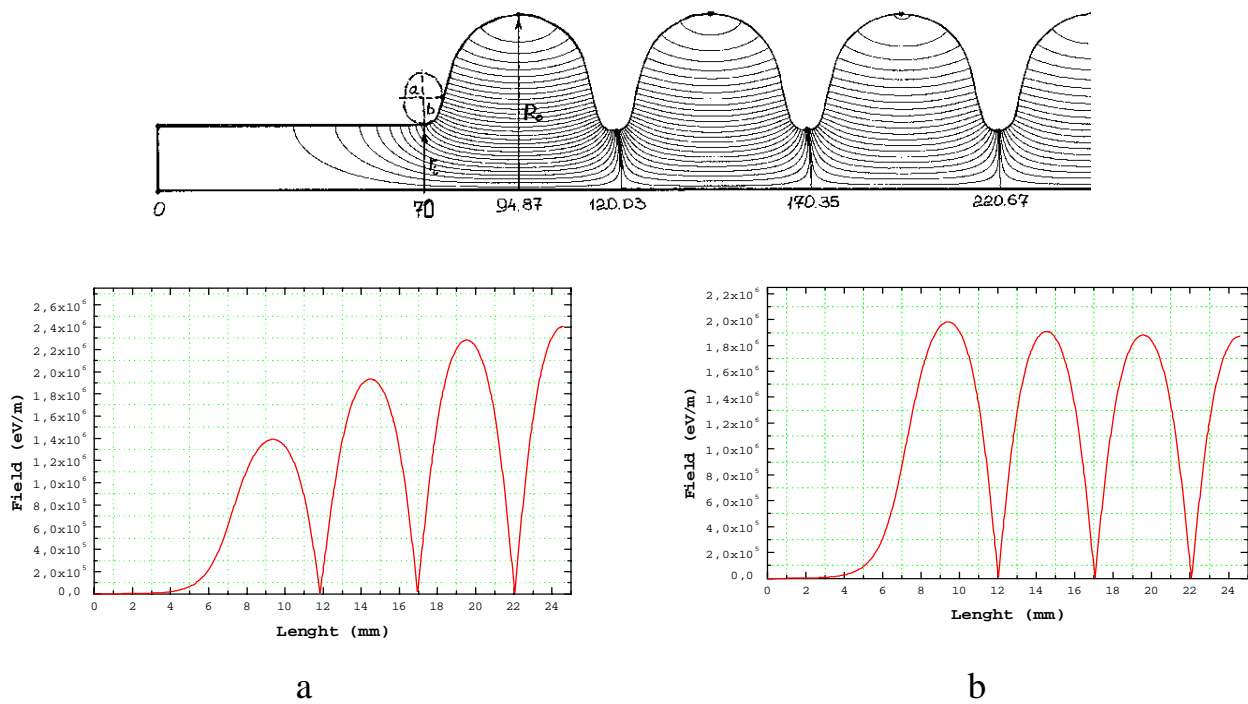


Fig.3. Electric field distribution on the axis of the half subcavity with the large beam pipe (calculated data)

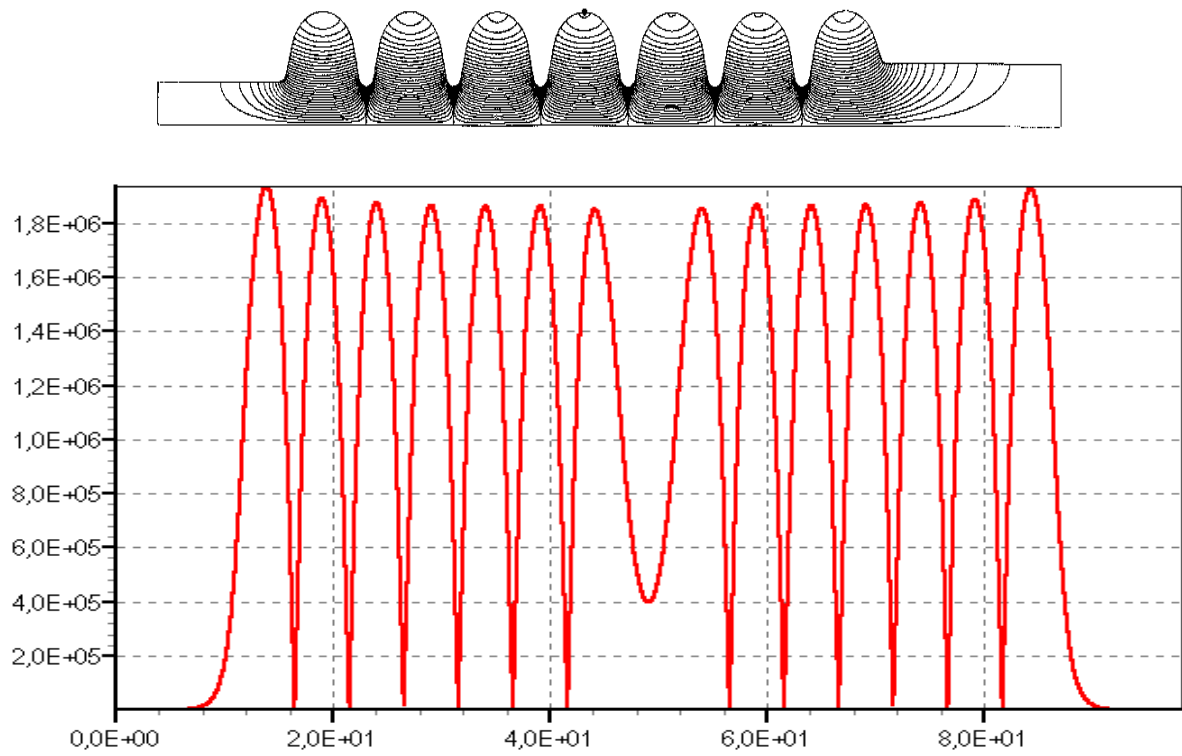


Fig.4. Electric field distribution on the axis of the two subcavities (calculated data)

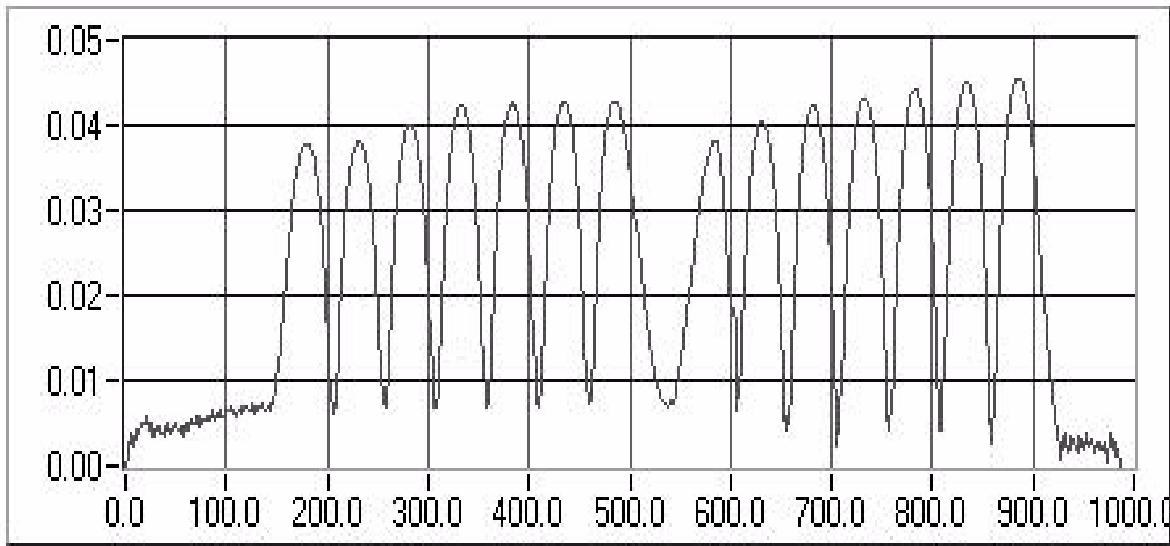


Fig. 5 Electric field distribution on the axis of the two subcavities
(measured data)

3. First variant of the test module.

First variant of the set-up (see Fig.6) consists of two subcavities, coupling with the feeding RWG through the beam pipe between them with diameter 34.02 mm and length $\lambda/4$. At another end of the subcavities there is the beam pipe with diameter 49.70 mm. Cut off frequencies of E_{01} mode in first and second beam pipes equal to 4615.98 MHz and 6746.44 MHz and field decay of -89dB/m and -154dB/m correspondingly.

It is known that external quality factor Q_{ext} does not depend on frequency scaling and in case of 2×7 -cells cavity it must be equal 0.8404×10^6 and for $2 \times 4 \times 7$ cells supercavity $Q_{\text{ext}} = 3.36 \times 10^6$ (for a fill time 0.5 ms). In the case of two cells coupled with the RWG coupler Q_{ext} must be 120000 [2]. We have considered two designs of RWG FM coupler to obtain this value of Q_{ext} . One of them (Fig.7 a) consists of $72 \times 13.08 \text{ mm}^2$ RWG short-circuited at the one end and coupled with two 7-cells cavities by the beam pipes with diameter 34.02 mm. The second FM coupler (Fig.7 b) differs a short-circuiting surface, which consists of cylindrical surface with diameter 42.739 mm and two plane surfaces tangential to the cylindrical one. An angle between two plane surfaces is equal to 63° . This set-up has dimensions of the input coupler corresponding to Q_{ext}

In the case of copper cavity at room temperature coupling coefficient χ of the cavity and input RWG $\chi \approx 0.0179$ ($Q_0 \approx 15000$) and input reflection coefficient is very close to 1. Field measurement device for these purposes realising of the nonresonant perturbation technique.

For the HOM damping we used the RWG with dimensions $48 \times 5 \text{ mm}$ inside the plunger, which may be moved in the RWG with dimensions $72 \times 13 \text{ mm}$. The position of the moving plunger was chosen to get the necessary value

of Q_{ext} . The waveguide, inserted in the plunger, was to cut-off the fields at the operation frequency (cut off frequency of $48 \times 5 \text{ mm}^2$ RWG is equal to 3.122838 GHz) and it permitted to propagate some HOM. Fig.7 shows a such type of the HOM damper.

Another type of HOM damper consists of three RWG with dimensions $48 \times 8 \text{ mm}^2$ coupled with beam pipe connecting neighboring cavities in the supercavity. Axes of two RWG create angle 90° and are terminated by the matched loads. Third RWG is short circuited and it's axis create 135° angle with respect to the axes of the other RWG. Such type of HOM damper is shown in Fig.8. This type of damper provides HOM damping for both polarization. Short circuiting plunger is used to increase HOM damping.

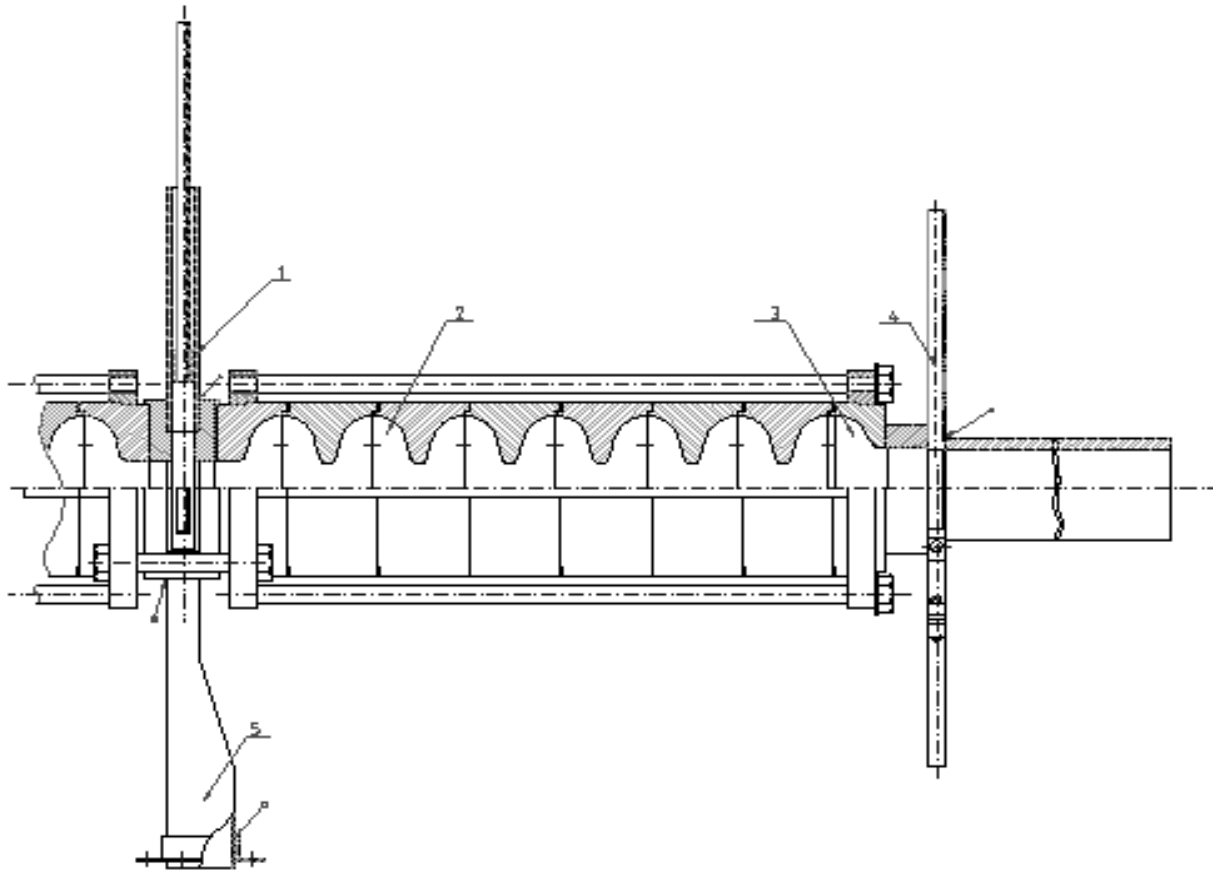


Fig. 6. TESLA S-band test module (first variant).

- 1.-moving short plunger with open for HOM withdrawing,
- 2.-cavity,
- 3.-ends cell with drift tube,
- 4.-HOM coupler,
- 5.-FM coupler.

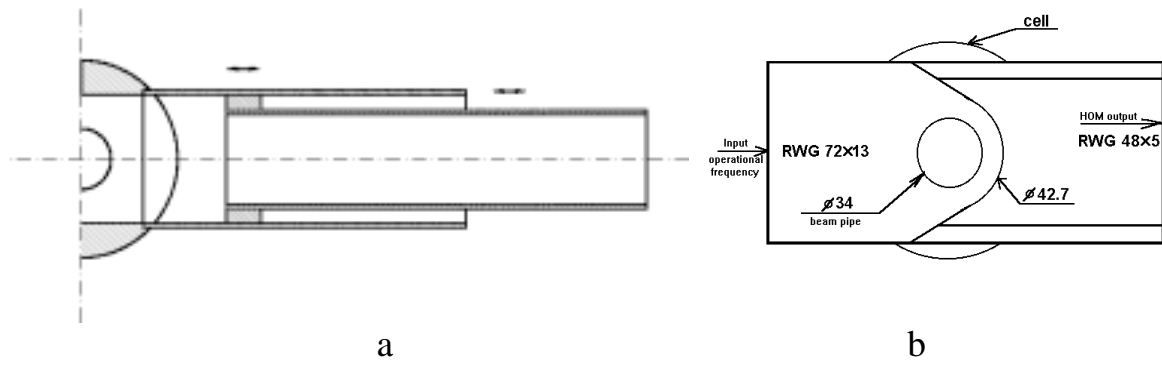


Fig.7. FM coupler with HOM damper

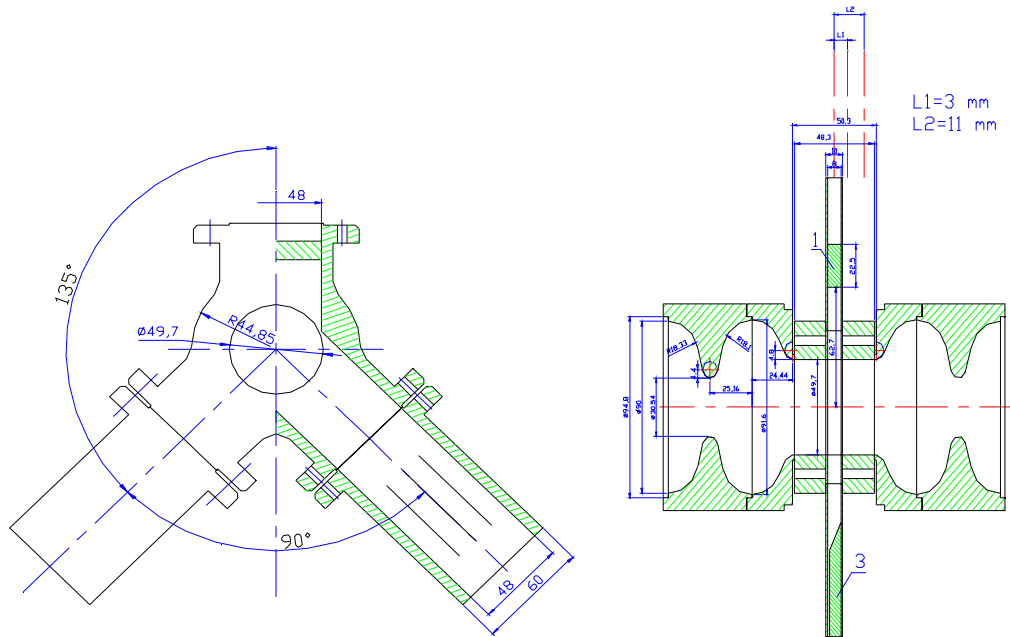


Fig.8 . RWG HOM coupler with slots orientated along beam pipe axis (with azimuthal slots)

Our latest experimental investigations show that this disposition of waveguide slot placed perpendicularly to drift tube axis (azimuthal slots) was't effective for withdrawing of HOM. We offer another construction, described below.

4. Second variant of the test module.

This variant differs from previous firstly by disposition of the RWG FM coupler. It was placed in the beginning of two subcavities coupling one with another through the beam pipe diameter 49.70 mm (Fig.9). For the HOM damping we have considered two RWG with dimensions 46x12 mm² attached to the beam pipe diameter 49.70 mm through the slots placed along beam pipe axis (longitudinal slots-Fig.10 and Fig.11a.). We decided to investigate this construction of HOM couplers, because our previous variant with azimuthal slots can't damping HOM effectively. Really, dipole HOMs exited in the 4×7 cells supercavity create H₁₁ like fields in the beam pipes connecting subcavities. For this beam pipe mode the ratio H_{z,max} component and H_{φ,max} component is

$$\frac{H_{z,\max}}{H_{\phi,\max}} = \frac{v_{11}^2}{\sqrt{(kR)^2 - v_{11}^2}} \quad (1)$$

where $k=\omega/c$, R is radius of the beam pipe, v_{11}' is the first root of the first derivative of the Bessel function J₁(x).

One can see that this ratio is more than 1 in wide frequency range(see Fig.13), and wide side of the rectangular waveguides must be orientated along the beam pipe. RWGs in this coupler have a strong coupling with dipole modes, provide strong damping and there is no coupling with the fundamental mode and other monopole modes.

But this construction with longitudinal slots has one disadvantage. It is difficult to install the RWG wide side between two cavities, because the beam pipe length is less, than its dimension. Therefore we had to use waveguide transition or the construction of two rectangular waveguide with dimensions 46x10 mm² and the slots by some angle to beam pipe axis (see Fig.11b).

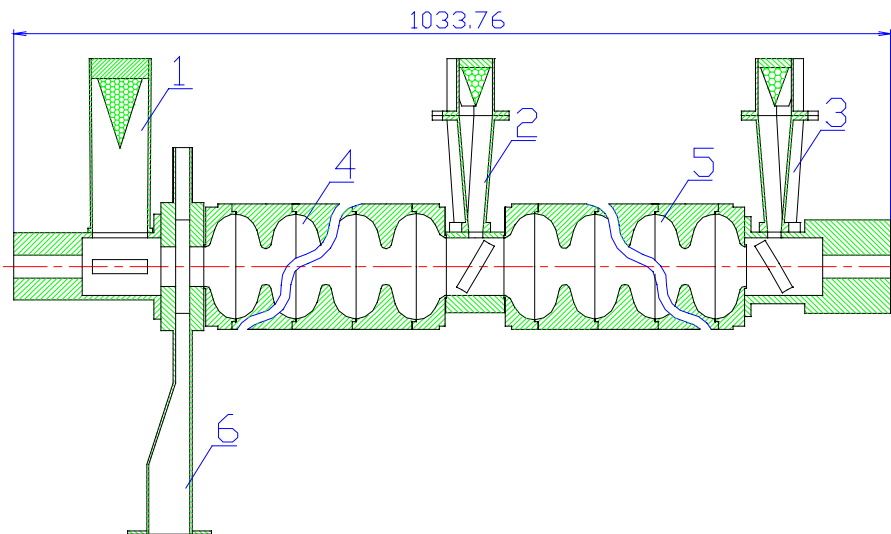


Fig.9. TESLA S-band test module (second variant).
1,2,3-HOM couplers; 4,5-cavities; 6-FM coupler.

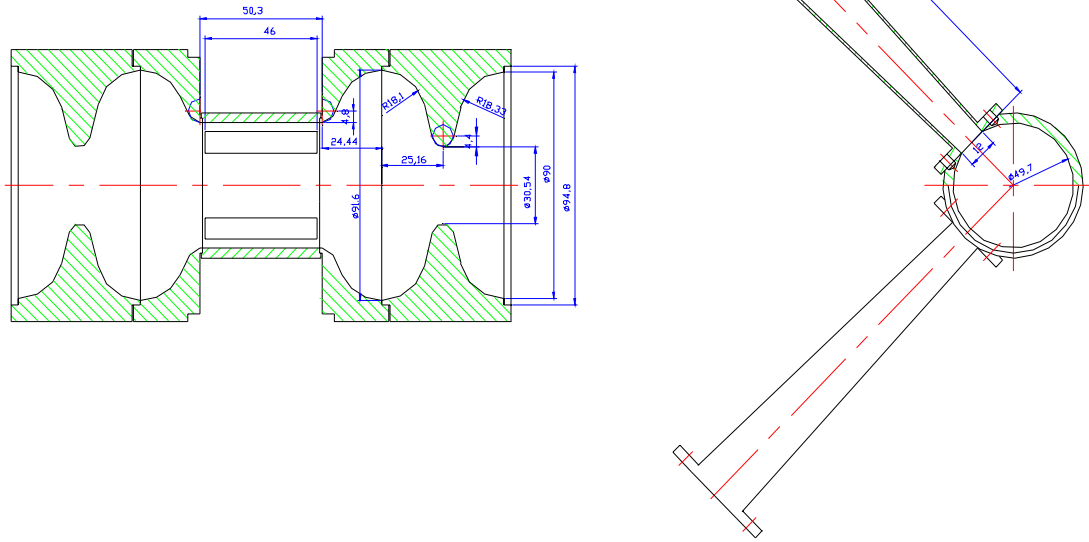


Fig.10. RWG HOM coupler with slots orientated perpendicular to beam pipe axis (longitudinal slots).

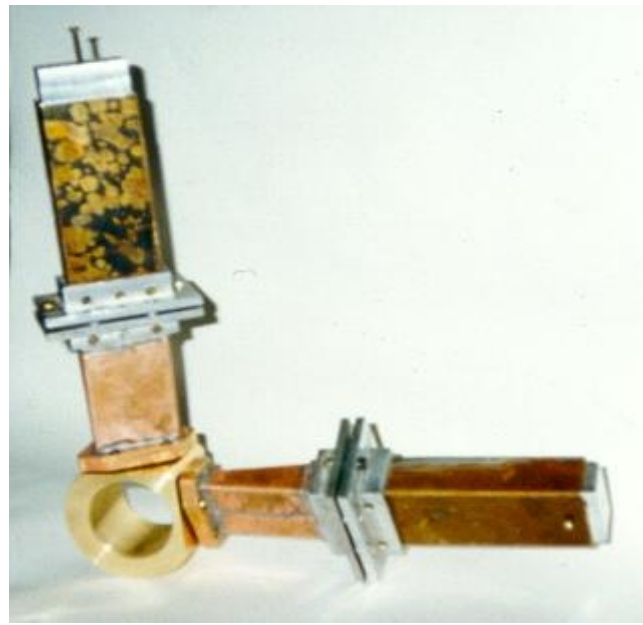


Fig.11. RWG HOM couplers.

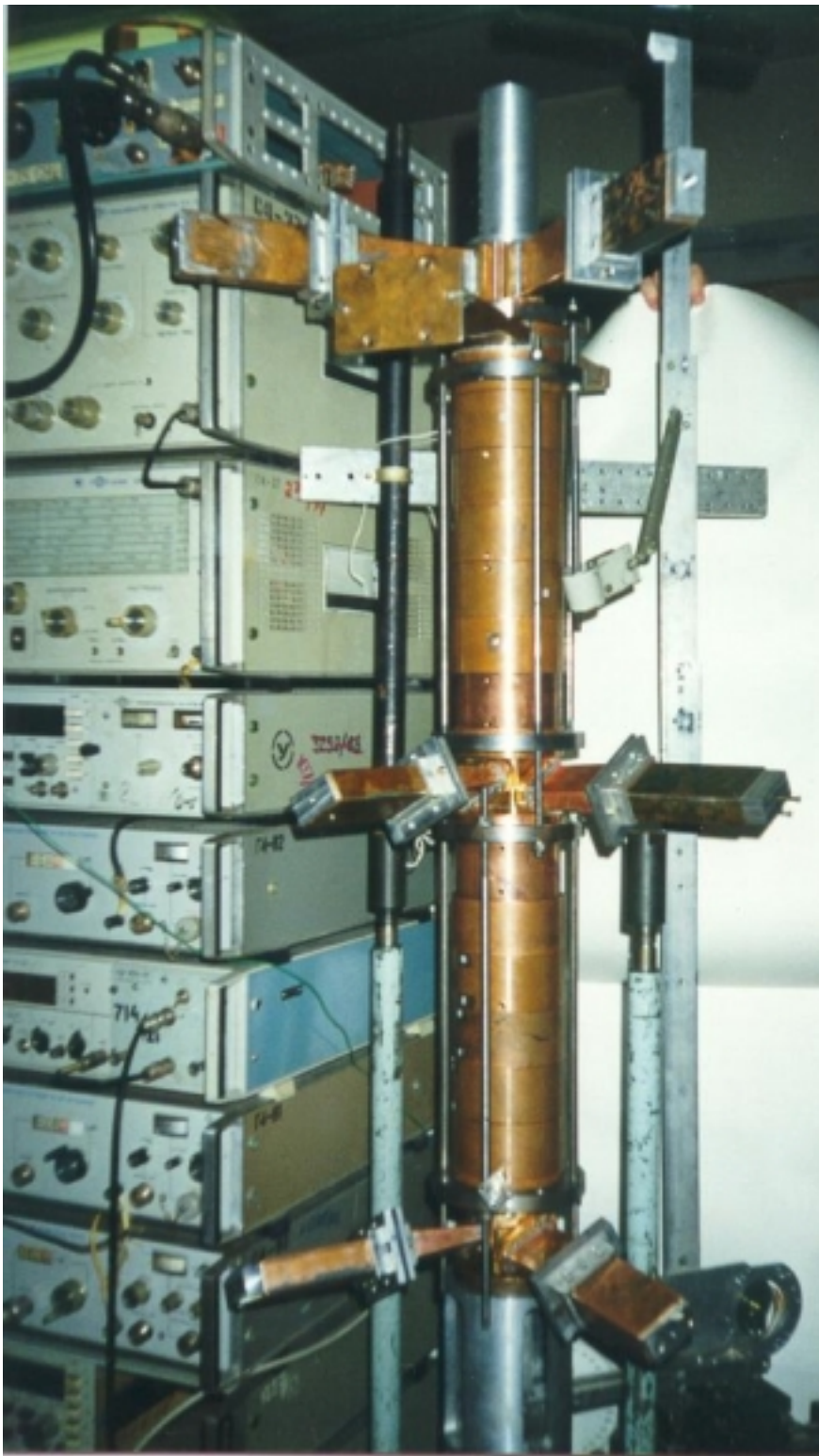


Fig.12. TESLA S-band test module.

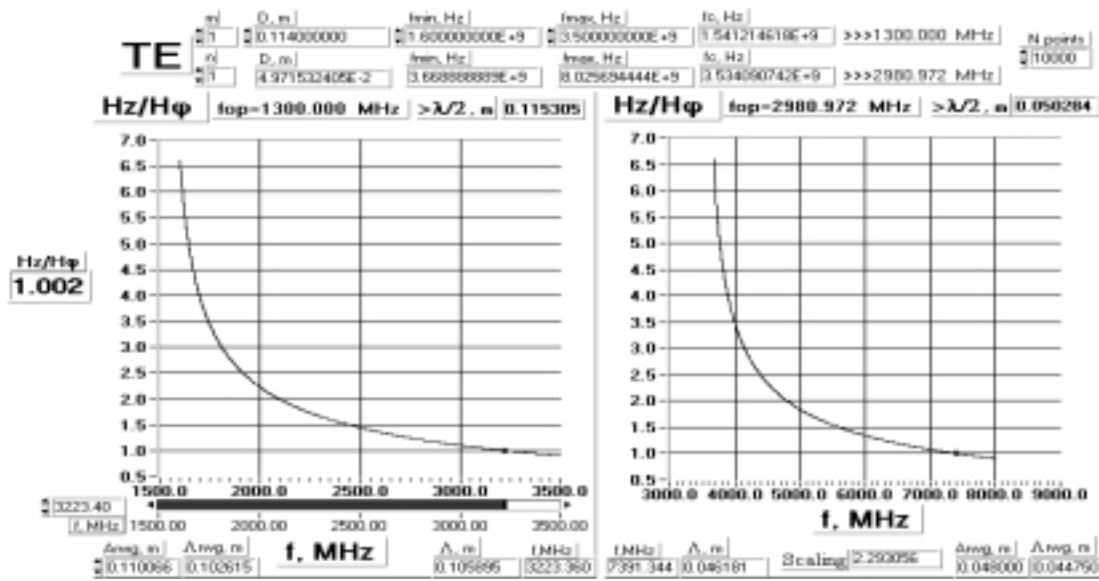


Fig.13. The dependence of the ratio component $H_{z\max}$ to $H_{\phi\max}$ on the surface of the beam pipe on frequency.

5. The investigations of high order modes.

In order to restrict the multi-bunch phenomena due to wakefields, the higher order modes of the TESLA cavity must be damped down to the certain Q_{ext} level. To estimate Q_{ext} we can use the following expression for the voltage induced by the train of $n-1$ bunches before the n -th bunch passage through the cavity

$$U_n = 2K_{\text{loss}} q_b \frac{1}{T_b/\tau} \left[1 - e^{-(n-1)T_b/\tau} \right] \quad (2)$$

where q_b is bunch charge; $T_b = 1/f_b$, f_b is a bunch repetition frequency;

K_{loss} is loss parameter of the considered HOM; $\tau = Q_{\text{ext}} / (\pi f_{\text{HOM}})$ is time decay of this HOM; f_{HOM} is a frequency of HOM. This expression corresponds to synchronization between HOM and train of bunches. In our case $f_b = f_{\text{op}}/920$, $f_{\text{op}} = 1.3\text{GHz}$ is operational frequency of the fundamental accelerating mode.

One can see that

$$A = U_{\infty} / 2K_{\text{loss}} q_b = \frac{e^{-T_b/\tau}}{1 - e^{-T_b/\tau}} \quad (3)$$

where A is maximum voltage induced by the infinite train of bunches, normalised to the voltage caused by a single bunch. The Q_{ext} level must be limited by the value

$$Q_{ext} \leq \pi f T_b \quad (4)$$

to avoid a resonant build up of U_n above $A2k_{loss}q_b$.

Fig.14 shows $U_n/(2K_{loss}q_b)$ dependence on bunch number n and Q_{ext} dependence on HOM frequency for $A=2$. One can see that the higher order modes of the TESLA cavity must be damped down to the Q_{ext} level of $10^4 - 10^5$. The external Q-factor do not depend on frequency scaling, material and temperature. Thus Q_{ext} measured in our frequency band must be the same as Q_{ext} measured in TESLA frequency band.

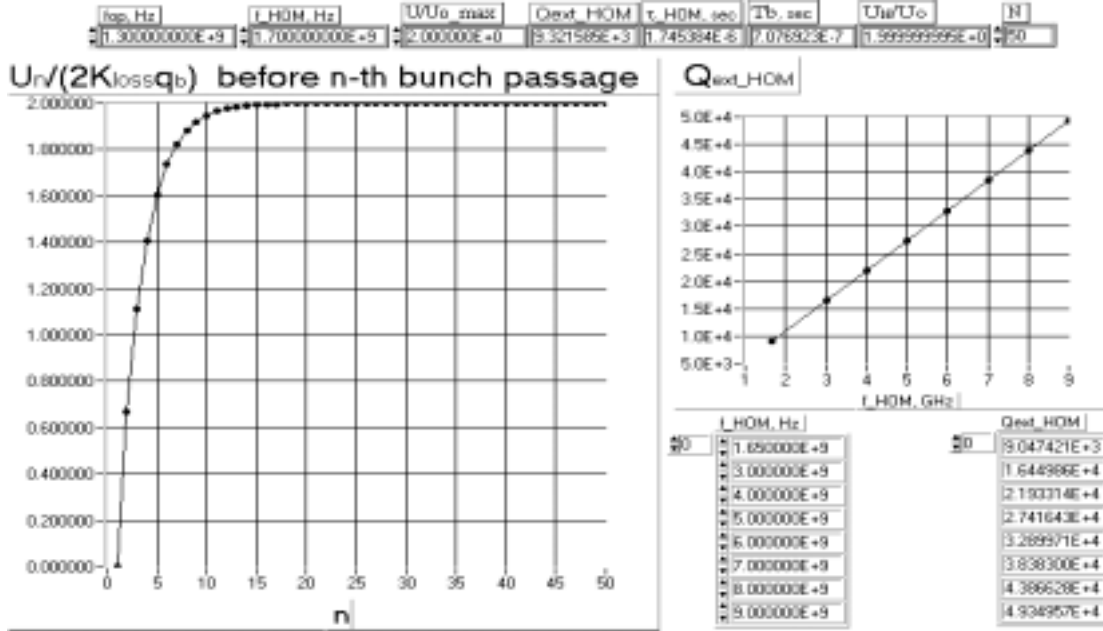


Fig.14 Normalized HOM voltage dependence on the bunch number and Q_{ext} dependence on HOM frequency for $A=2$.

We have determined the Q_{ext} for different RWG HOM coupler, using the results of quality factor measurements for the two cavities with beam pipe and without HOM coupler (measuring Q_1 , see Fig.15a) and with HOM coupler (measuring Q_2 , see Fig.15b). The external Q-factor may be calculated now from

$$Q_{ext} = Q_1 Q_2 / (Q_1 - Q_2) \quad (5)$$

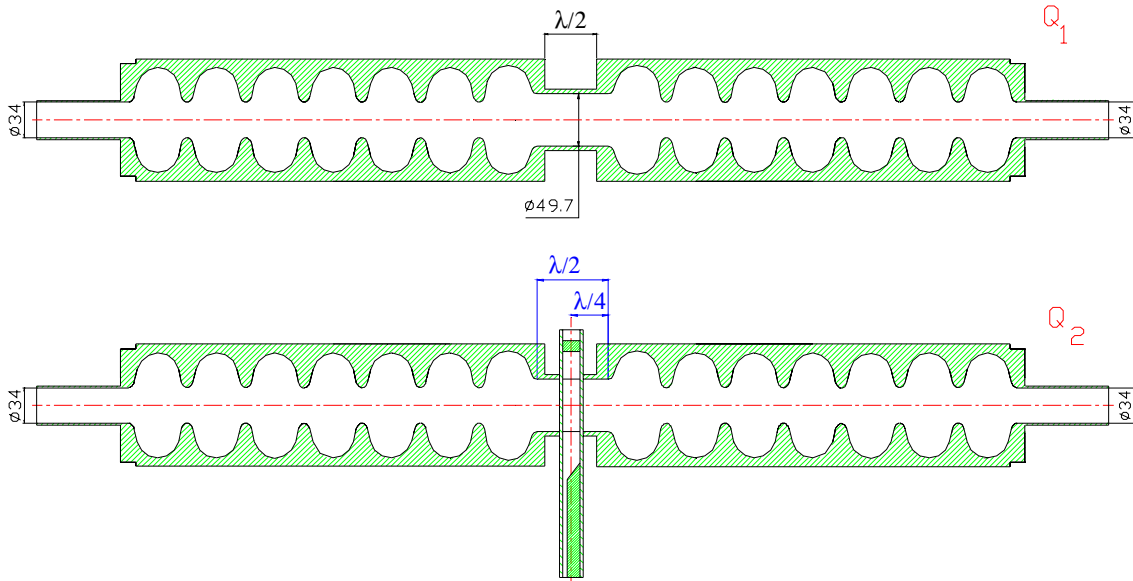


Fig.15. Set-up for determination of the external quality factor

We carried out research of three HOM couplers. The HOM couplers represent in all cases RWG with the sizes $48 \times 8 \text{ mm}^2$, connected with beam pipe and terminating by the absorbing load. Two RWG, revolved on 90° from each other around of an axis of the beam pipe were used for withdrawing HOM. Thus the wide wall RWG in one case was guided perpendicularly axes of the beam pipe, in the other cases –parallel to axis, and in the third case-under a corner 60° to an beam pipe axis.

The results of measurements for all three HOM coupler are summarized in Table 2 and Table 3. The asterisk * marks those HOM, for which $Q_1=Q_2$. Dash designates absence of excitation at presence appropriate HOM coupler.

Appendix 2 shows E_z component distribution along the cavity axis for H_{111} and E_{110} modes in two subcavities, connected one with another by beam pipe with length $\lambda/2$ and short-circuited at the ends beam pipes. These pictures are the example of experimental investigations of HOM with using of bead pulling technique.

In Table 4. the data for two coaxial HOM coupler, connecting with single nine cells cavity of TESLA are given. As it is visible from comparison these two Tables RWG HOM coupler provides required withdrawing HOM in the superstructure.

Table 2. Comparison RWG HOM couplers.

HOM	Frequency, MHz		$Q_0 \times 10^3$	$Q_{ext}, 10^3$		
	Model	TESLA		HOM coupler type.		
				\perp axb=46x 12mm see Fig.8	II axb=46x 12 mm see Fig.10	// axb=46x 10mm see Fig.11
H ₁₁₁	3744.47	1632.90	9.6	451	17.5	48
	3784.07	1650.20	8.1	*	2.0	18
	3840.13	1674.65	12.8	260	-	13.6
	3843.10	1675.94	7.0	*	1.75	9.9
	3918.58	1708.89		*	-	-
	3922.84	1710.75		36.0	5.44	5.44
	4000.60	1744.62	10.2	*	-	0.74
	4009.21	1748.37	11.5	209	32.6	7.9
	4074.72	1776.94	10.1	*	-	0.6
	4089.85	1783.54	11.6	180	13.8	5.0
E ₁₁₀	4127.07	1799.77	10.2	105	-	3.1
	4131.77	1801.92	9.9	*	17.7	15.9
	4229.48	1843.60	16.9	*	-	1.3
	4233.52	1845.99	16.3	*	7.6	19.6
	4269.37	1861.59	15.7	*	-	1.1
	4273.83	1863.61	12.2	*	20.1	37.4
	4298.55	1874.40	16.7	*	-	15.3
	4302.03	1875.92	16.8	*	38.6	124
	4317.11	1882.60	14.5	*	2.1	2.9
	4319.46	1883.60	15.7	*	2.1	29.9
	4327.33	1887.32	16.7	*	3.1	4.1
	4330.72	1888.58	14.7	*	-	*
	4332.00	1889.18	14.5	90.6	4.9	10.8

Table 3. Comparison RWG HOM couplers for E₀₁₁ mode.

Frequency F, MHz	Q ₀ ×10 ³	 axb=46x10 MM see Fig. 10		⊥ axb=28x12. 5 MM see Fig.8		+⊥+ - axb=46x12 mm ⊥- axb=28x12. 5 mm	
		Q _L × 10 ³	Q _{ext} × 10 ³	Q _L × 10 ³	Q _{ext} × 10 ³	Q _L × 10 ³	Q _{ext} × 10 ³
5481.83	15.4	14.5	248.1	12.7	72.44	14.7	323.4
5502.40	5.1	4.7	59.9	4.75	69.2	4.7	59.92
5509.82	11.9	8.9	35.3	5.55	10.4	8.7	32.35
5539.50	9.0	5.9	17.13	3.85	6.73	4.73	9.97
5577.20	9.7	4.6	8.75	3.35	5.12	2.53	3.42
5599.93	12.4	5.0	8.38	-	-	-	-
5618.70	11.2	3.4	4.88	2.5	3.22	1.73	2.05
5633.00	14.0	-	-	-	-	-	-
5643.90	14.5	4.1	5.72	4.0	5.52	1.86	2.13

The RWG HOM coupler does not need the rejection filter, which is required by the coaxial HOM coupler to avoid the damping of the fundamental mode. This is because the RWG below cut-off on the operation frequency, and HOM coupler with a wide wall, guided parallel of beam pipe axis, do not cooperate at all with an operation frequency of the cavity. Besides this HOM coupler provide rather strong connection with dipole modes of the subcavity, as longitudinal component of the magnetic field in the beam pipe in 3-6 times surpasses the azimuthal component on the beam pipe surface.

The opportunities considered three HOM couplers were investigated also on the S-band model consisting of two half-cells, connected of beam pipe of $\lambda/4$ and diameter of 49.7 mm. The half-cells were identical also their sizes corresponded to the sizes of a final cell. The HFSS program was used to calculate the resonance frequency and Q-factor for this model without and with HOM couplers. In Table 5 there are the calculated data with HFSS program. The frequencies f_1 were calculated for model without HOM couplers and f_2 and f_3 are the frequencies for model with transverse rectangular waveguide of HOM coupler and for HOM coupler with waveguide at angle 70° to the beam pipe axis correspondingly. In last case the waveguides were disposed at 5 mm from the beam pipe center in longitudinal direction.

Table 4. Withdrawing of HOM by coaxial HOM couplers (both polarisation)

	HOM	TESLA f, MHz	$Q_{\text{ext}}(\times 10^3)$
H ₁₁₁	1	1622.2	20.3-193.0
	2	1622.3	14.4 – 366.0
	3	1629.8	48.0-68.7
	4	1629.9	39.4-77.0
	5	1642.3	25.0
	6	1642.2	23.6-37.0
	7	1659.1	16.1-42.0
	8	1660.3	12.2-22.0
	9	1681.2	9.3-11.0
	10	1682.2	8.5-23.0
	11	1706.7	4.8-5.9
	12	1707.8	5.5-8.1
	13	1734.0	3.4-6.1
	14	1734.3	4.3-4.5
	15	1762.1	2.7-6.0
	16	1762.2	3.2-3.9
	17	1786.5	2.1-4.6
	18	1789.4	2.8
E ₁₁₀	1	1799.9	5.2
	2	1800.9	3.0-4.2
	3	1837.0	19.8-29.8
	4	1835.7	18.6-18.9
	5	1852.7	27.0-27.7
	6	1853.2	20.9-27.5
	7	1865.3	30.6-50.6
	8	1865.5	26.5-50.6
	9	1874.4	50.2-66.6
	10	1874.8	51.1-56.5
	11	1880.8	93.6-95.1
	12	1881.2	76.1-85.5
	13	1885.2	18.1-123.4
	14	1885.4	75.2-204.8
	15	1887.4	170.1-633.0
	16	1887.8	251.0-341.2
	17	1889.1	459.9-1800.0

Table 5. Calculated data with HFSS program of HOM coupler between two half cells.

f ₁ , MHz	⊥			
	f ₂ , MHz	Q	f ₃ , MHz	Q
3617	3992	79	3547	21
3946	4449	1780	3986	80
4452	5037	17	4438	111
4891	5426	226	5031	15
5384	5706	300	5381	307
5686			5426	271
			5686	178

Two polarization of dipole modes were obtained during the calculations. The Q values were difficult to be calculated of them small values, when HOM couplers were used, and therefore it was overlapped of the amplitude-frequency dependencies. The experimental definition of this value was aggravated also by difficulty of identification of modes.

In the appendix 3 the results of measurements of a electric field longitudinal component distribution are given for the model without and with HOM couplers. The measurements were carried out on off the axis. As allows from these data, the effective coupling HOM coupler with waves in the beam pipe depends on the location of the coupling slots concerning the pipe center. Obviously, optimum variant for the withdrawing HOM is the displacement HOM couplers from the pipe center.

6. RWG HOM couplers in TESLA cryostat

Let's consider the possibility to arrange the RWG HOM coupler in TESLA cryostat [3]. How it was pointed out these HOM coupler must damp in frequency band 1300 MHz - 2980.72 MHz how dipole and also monopole HOMs and do not be coupled with the fundamental mode We considered two variants of RWG HOM couplers.

Three RWG HOM coupler.

It shows at Fig.16. This RWG HOM coupler consists of three RWG. Two 110×20 mm² RWG damp dipole HOMs and 70×20 mm² RWG damps monopole HOMs. To decrease longitudinal dimension we use tapered waveguide transitions from 110 mm to 95 mm and from 20 mm to 10 mm. All transitions have 70 mm length. The longitudinal position of 110×20 mm² RWG was chosen due to following reason. The lowest dipole HOMs excite H₁₁-like electromagnetic field in the beam pipe tube. At the frequencies of these HOMs

the ratio $H_z/H_\phi = 2.5 - 6.5$. Thus H_z component of the magnetic field provides strong coupling of lowest dipole HOMs with H_{10} mode. in RWG

Two $110 \times 20 \text{ mm}^2$ RWG are rotated through 90° from each other around of on axis of the beam pipe to withdraw dipole HOM of both polarizations. These RWG are strongly isolated against fundamental and other monopole modes and don't require any tuning. This is the main advantage of the RWG HOM couplers compared to coaxial ones. They have cut off frequency 1362.7 MHz for wide wall $a = 110 \text{ mm}$ and 1577.9 MHz for $a = 95 \text{ mm}$. Such parameters provide good transmission at the lowest dipole mode frequencies.

The third RWG with dimensions $70 \times 20 \text{ mm}^2$ has cut off frequency 2141.4 MHz. This RWG is used for withdraw monopole HOMs. It has some coupling with fundamental mode.

Fig.17 and Fig.18 show RWGs location in the cryostat. The beginning part of each RWG (from beam pipe tube to flange) is made of Nb and is superconducting (2°K) and has a length of 90 mm. The final part of each RWG is made of stainless steel covered by copper. The wall thickness of steel RWG is equal to 0.2 mm and the length is about 1 m. These waveguides are terminated by the matched loads, which have 70°K temperature.

Under these conditions heat flux from the 70°K region to 2°K region can be estimate.

$$P = \frac{A}{L} \int_{T_1}^{T_2} K(T) dT, \quad (6)$$

where A is stainless steel RWG cross section area, L is RWG length, K(T) is stainless steel heat conductivity, $T_1 = 2^\circ\text{K}$, $T_2 = 70^\circ\text{K}$.

Estimation gives 13mW for $110 \times 20 \times 0.2 \times 1000$ RWG and 9mW for $70 \times 20 \times 0.2 \times 1000$ RWG.

Let us estimate heat loading for 70°K region provided by the HOM's wave. We used the following formula

$$P_{beam} = K_{loss} q^2 f_{bunch} T_{cur} f_{rep}, \quad (7)$$

where

$q = 5.8 \times 10^{-9} \text{ C}$ is bunch charge,

$f_{bunch} = f_{op}/920$ is bunch repetition frequency,

$f_{op} = 1300 \text{ MHz}$ is operational frequency,

$T_{cur} = 0.762 \text{ ms}$ is current pulse duration,

$f_{rep} = 5 \text{ Hz}$ is pulse repetition rate,

$K_{loss} = \frac{\omega_{mod} e R}{4 Q}$ is loss parameter of some mode.

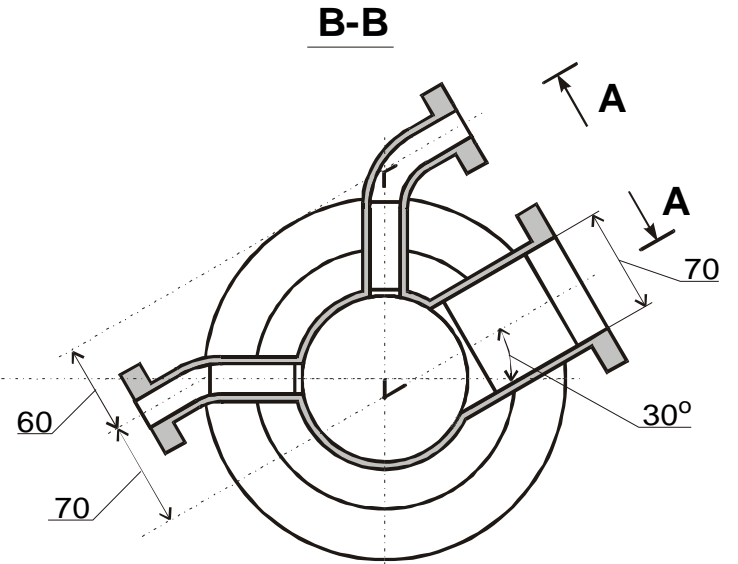
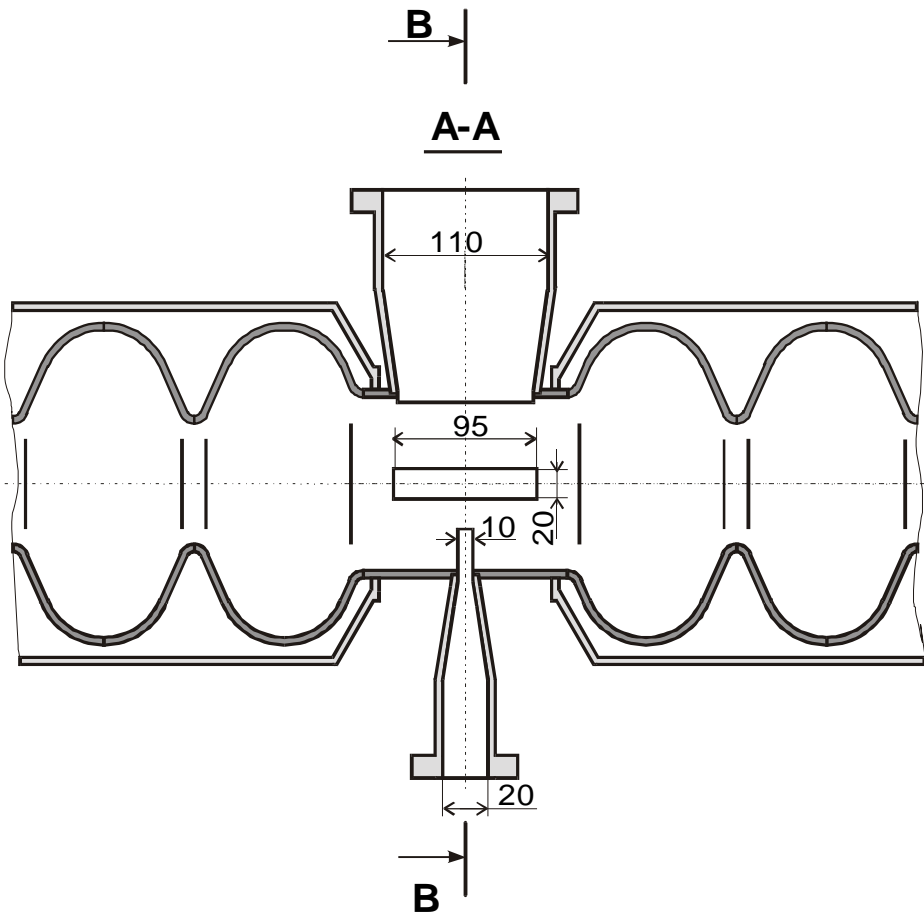


Fig. 16. Three RWG HOM coupler.

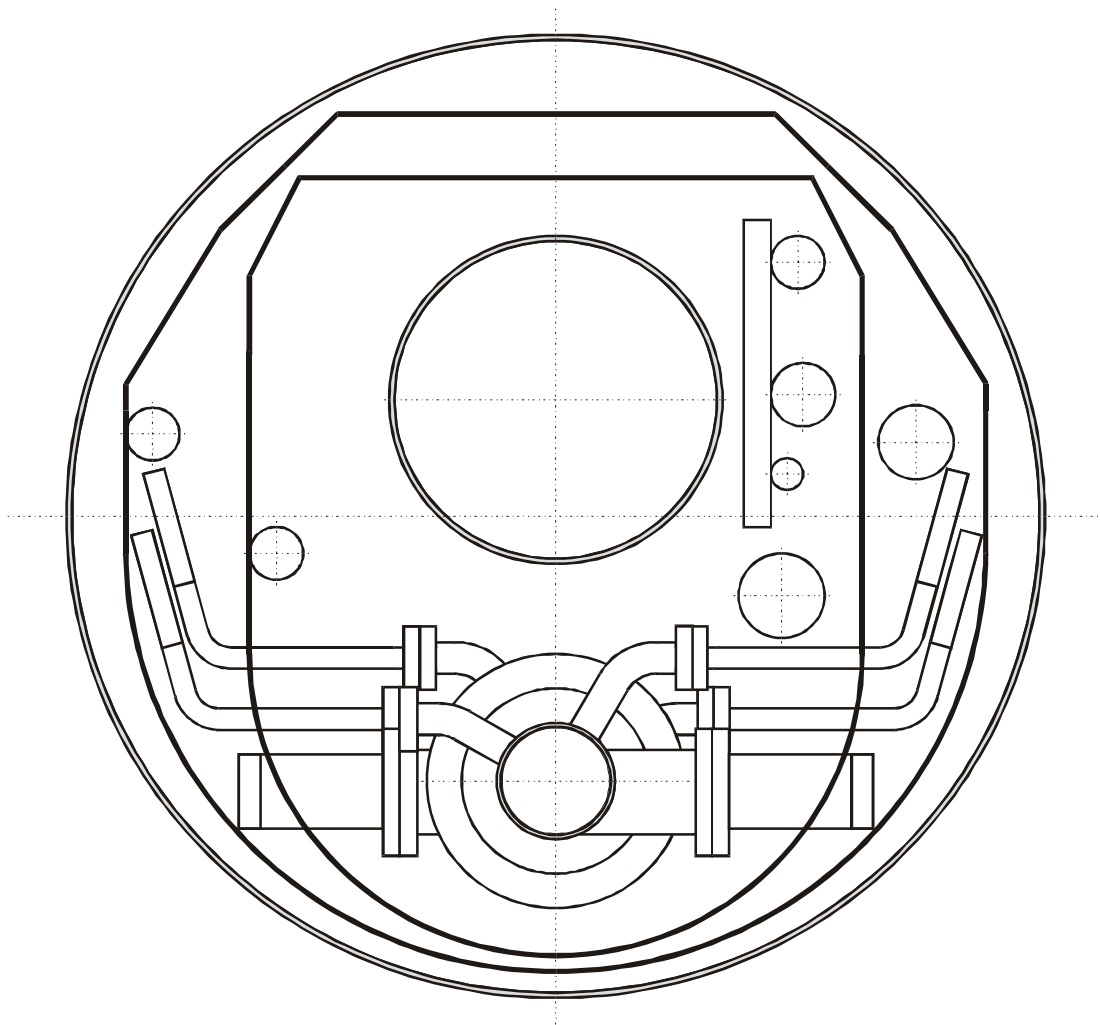
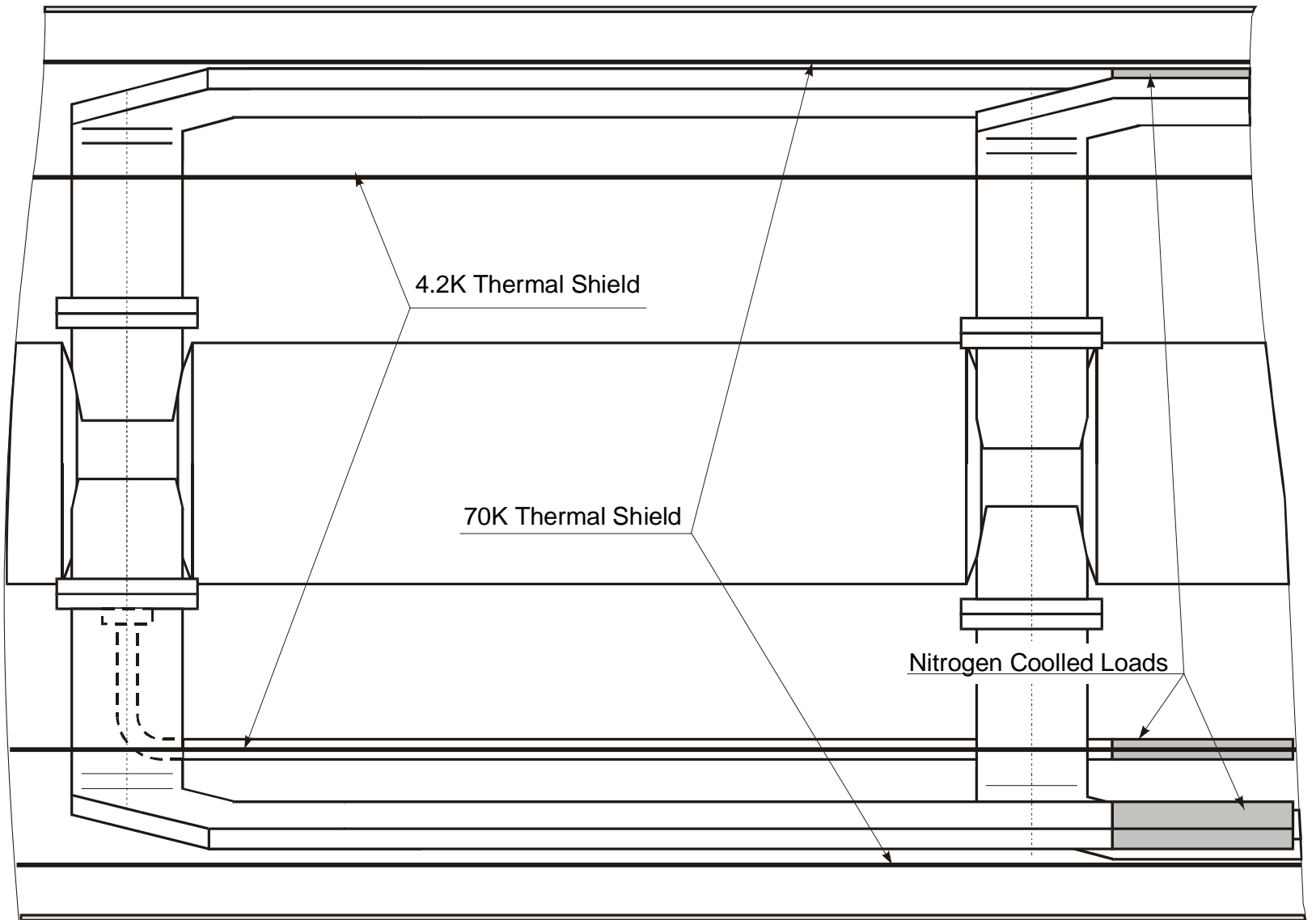


Fig.17. Three RWG HOM coupler location in the cryostat.
Front view.

Fig. 18. Three RWG HOM coupler. Top view.



The calculation data are presented in the Table 6 and Table 7. The R/Q values were taken for 9-cell cavity from [1]. The Table2 data correspond to bunch displacement of 1 cm from the cavity axes.

Let us point out heat flux from 300°K region to the 70°K region through a 1 m long stainless steel RWG is equal to 2×0.146 W for two 110×20 mm² RWGs and 0.101 W for one 70×20 mm² RWG. It shows that matched loads location in the 70°K region is preferable.

Table 6. Monopole modes withdraw through 70×20 mm² RWG.

Mode	Frequency, MHz	R/Q, Ohm	K_{loss} , V/C	$P_{\text{beam av}}$, mW
E ₀₁₁	2438.7	6.93	2.7×10^{10}	4.8
	2448.4	67.04	2.6×10^{11}	46.8
	2454.1	79.5	3.1×10^{11}	55.7
E ₀₁₂	3845.3	22.04	1.3×10^{11}	24.2
	3857.3	6.85	4.2×10^{10}	7.5
Σ				139

Table 7. Dipole modes withdrawn through 110×20 mm² RWGs.

Mode	Frequency, MHz	R/Q, Ohm/cm ²	K_{loss} , V/C	$P_{\text{beam av}}$, mW
H ₁₁₁	1707	10	2.7×10^{10}	4.9
	1734	15.4	4.2×10^{10}	7.6
	1762	2.23	6.2×10^9	1.1
E ₁₁₀	1836	0.45	1.3×10^9	0.2
	1853	0.33	9.6×10^8	0.2
	1865	6.47	1.9×10^{10}	3.4
	1874	8.75	2.6×10^{10}	4.7
	1881	1.83	5.4×10^9	1.0
	1887	0.18	5.3×10^8	0.1
H ₁₂₁	3075	0.11	5.3×10^8	0.1
	3079	0.14	6.8×10^8	0.1
	3082	0.92	4.5×10^9	0.8
	3087	1.28	6.2×10^9	1.1
Σ				25.3

Let us estimate 70×20 mm² RWG heating due to fundamental mode losses under the following assumptions. For effective accelerating field

$E_{\text{eff}}=25$ MV/m maximum amplitude of the accelerating field on the cell axis is equal to $E_{z \text{ max}}=49.06$ MV/m. Then according to J.Sekutowicz's calculation electric field amplitude in the middle of the beam pipe with diameter 78 mm $E_{z \text{ tube}}=8.79$ MV/m ($E_{z \text{ max}}/E_{z \text{ pipe}}=5.58$), and magnetic field amplitude near the beam pipe surface can be estimated as

$H_{\phi \text{ tube}} \geq 7.82$ kA/m. In this case magnetic field parameters at the beginning of the RWG are $H_{x0} = H_{\phi \text{ tube}} = 7.82$ kA/m and $H_{z0} = 9.84$ kA/m. Fields decay as $\exp(-\alpha z)$, where $\alpha = 35.66$ 1/m. If repetition rate is equal to 5 Hz and current pulse duration is equal to 0.762 ms then average power dissipated in the nonsuperconducting RWG walls is equal to $P_{\text{Cu}} = 1.5 - 2.7$ mW. Thus full 2°K region heat loading is about 37 mW.

Of course, RWG is cumbersome but 1m long 110×20 mm² RWG has 400 grams mass due to thin walls.

It is necessary to point out the thin-wall stainless waveguide is mechanically deformable. It does not permit us to use these waveguides under condition when the pressure inside and outside of the waveguides is different. To protect possible deformations we recommend to use gas permeable stainless steel waveguide and vacuum windows located between superconducting part and stainless part of the RWG. The windows must be able to pass peak power of the order of some tens watts at the temperature of 2°K.

Two RWG HOM coupler.

Fig.19 shows two RWG HOM coupler. Its RWGs are rotated through 45° - 60°. It reduces the longitudinal RWGD size and permits coupling with both monopole and dipole HOMs including fundamental mode. Two 110×20 mm² waveguides are rotated through 90° one relative another to damp dipole HOM of both polarization.

Let us estimate 110×20 mm² RWG heating due to fundamental mode losses under the following assumptions. Superconducting part of the RWG has length of 430 mm and nonsuperconducting part (steel covered by copper) has 570 mm length (full length is equal to 1000 mm). Under these conditions estimated heat flux from the 70°K region to 2°K region is equal to 23.3 mW for $110 \times 20 \times 0.2 \times 570$ stainless steel waveguide. Effective accelerating field is $E_{\text{eff}} = 25$ MV/m, accelerating field amplitude $E_{z \text{ max}} = 49.06$ MV/m, electric field amplitude on the axis of the beam pipe with diameter 78 mm $E_{z \text{ tube}} = 8.79$ MV/m, magnetic field amplitude nearly the beam pipe tube wall $H_{\phi \text{ tube}} = 7.82$ kA/m. In this case magnetic field parameters at the beginning of the RWG are $H_{x0} = H_{\phi \text{ tube}} \times \sin(60^\circ) = 7.82 \times \sin(60^\circ) = 6.77$ kA/m and $H_{z0} = 7.82 \times \cos(60^\circ) = 3.91$ kA/m. Here 60° is the angle between cavity axis and RWG wide wall. Fields decay as $\exp(-\alpha z)$, where $\alpha = 8.563$ 1/m. If repetition rate is equal to 5 Hz and current pulse duration is equal to 0.762 ms then average power dissipated in the nonsuperconducting RWG walls is equal to $P_{\text{Cu}} = 13.1 - 25.1$ mW.

It is necessary to point out the length of the RWG superconducting part is 5-6 times larger than in the three-RWG HOM coupler. It is because of the strong coupling of inclined RWG and fundamental mode field. We are forced to use such long superconducting RWG to provide a decay of the fields excited by the fundamental mode in the RWG. At the same time we are forced to put superconducting RWG in the 4°K region (as it is shown in Fig.20 and Fig.21). It creates additional problems in constructing of stainless steel RWG from the 4°K region to the 70°K region (stainless steel RWGs are not shown in Fig.20 and Fig.21). From this point of view three-waveguide RWGD is more preferable than two-waveguide one.

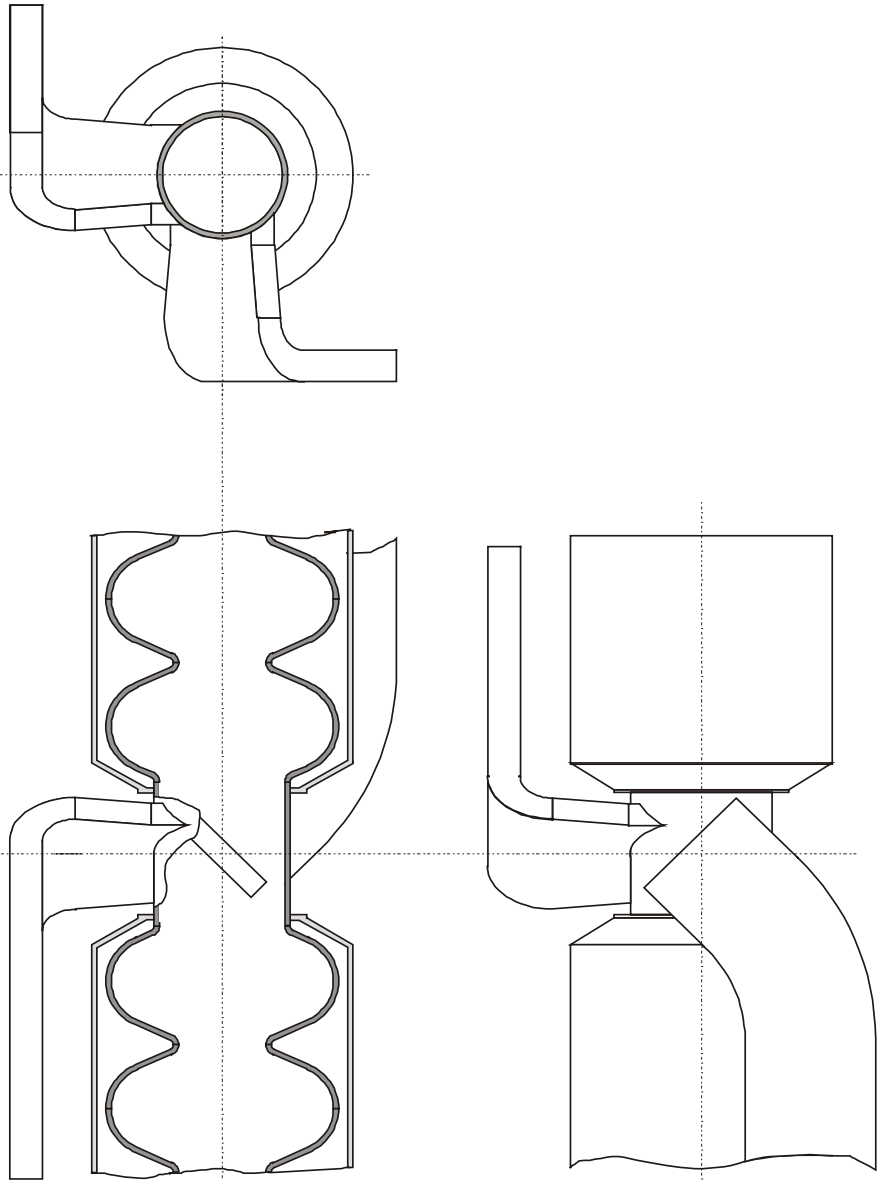


Fig.19. Two RWG HOM coupler

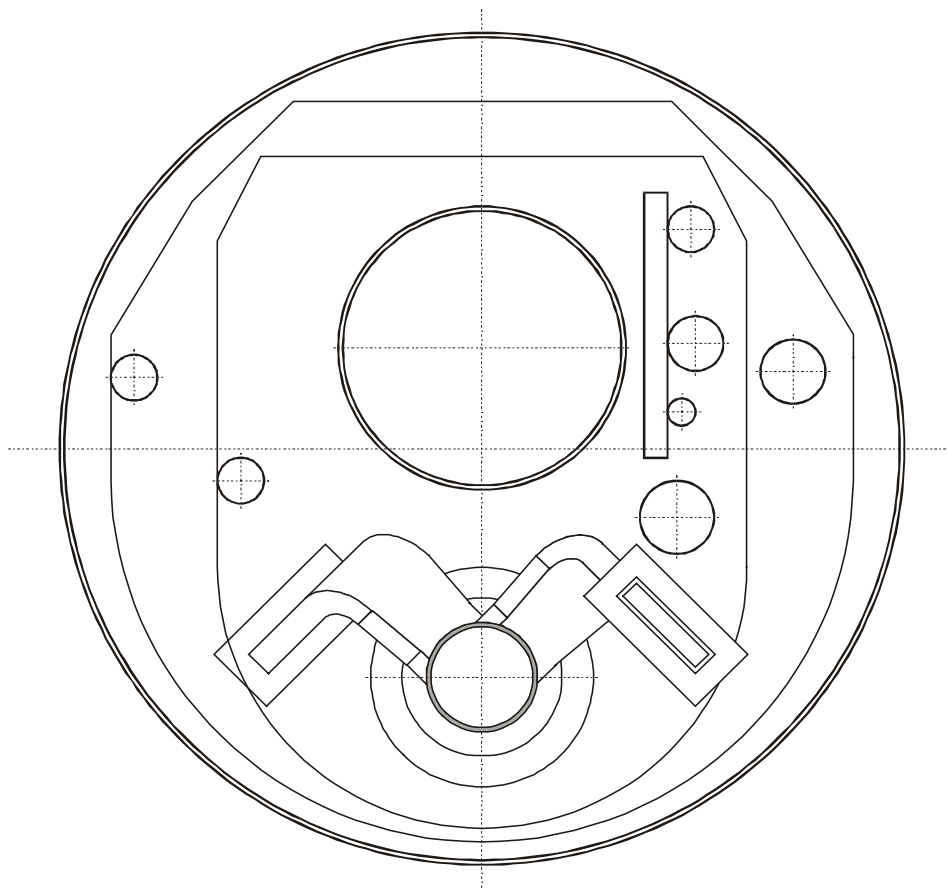


Fig.20. Two RWG HOM coupler. Front view.

Table 8. Heat loading of 2K region per 4×7 cells superstructure

	RWG dimensions a×b×t, mm ³	Nonsuper- conducting RWG length, mm	Static losses per one RWG 70K→2K, mW	Fundamental mode losses per one RWG, mW	Number of RWGs	Losses per super- structure, mW
Version 1	110×20×0.2	1000	13	0	2×4	148
	70×20×0.2	1000	9	2	1×4	
Version 3 45° , 30dB filter	110×20×0.2	1000	13	4	2×5	170

RWG HOM coupler version 2 is not included in the Table 8. This version is not competitive due to great constructive problems.

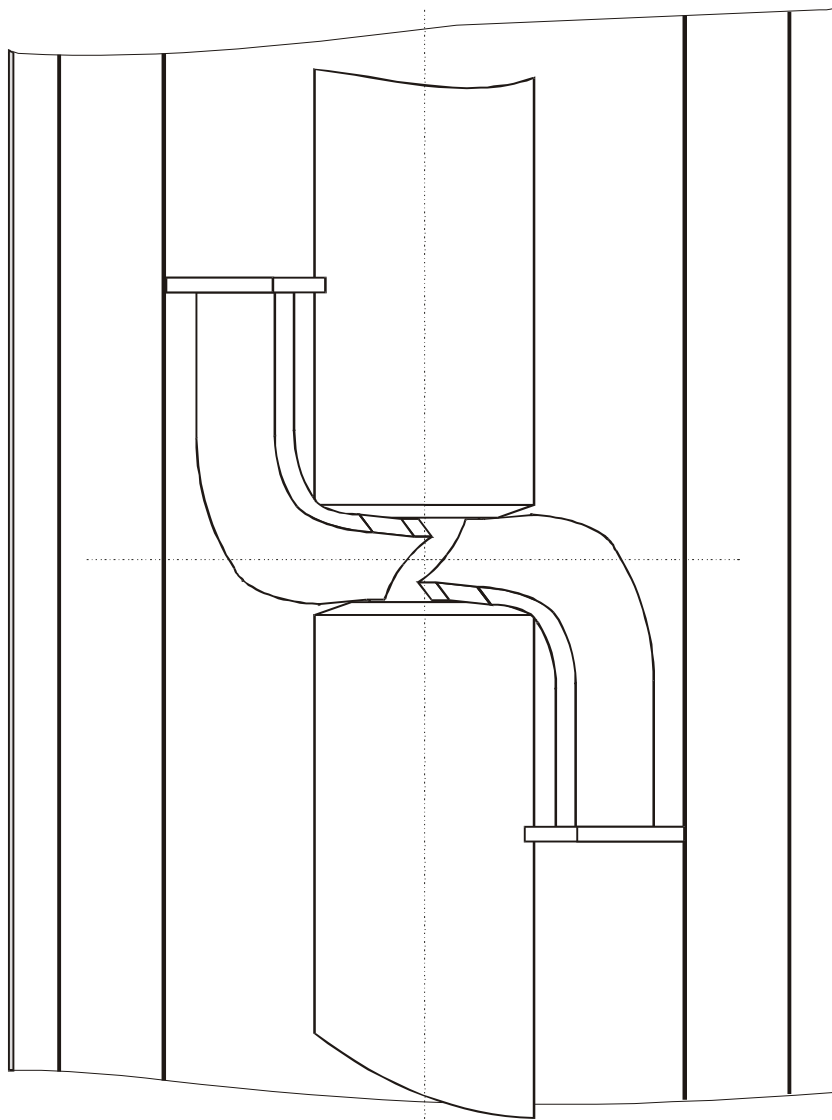


Fig.21. Two RWG HOM coupler. Top view.

The two RWG HOM coupler with superconducting rejection filter.

The strong coupling with fundamental mode field is a main disadvantage of the RWG HOM coupler discussed in the last partition. Let us consider variant of two-RWG HOM coupler with narrow-frequency band rejection filter tuned to resonate with fundamental mode fields. Approximate design of such filter is given in fig.23. The internal sizes of RWG are 110x20 mm

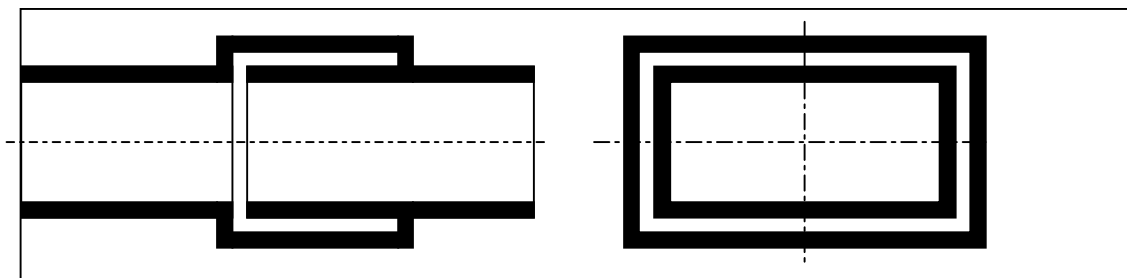


Fig.23. Narrow frequency band rejection filter.

Calculations carried-out with HFSS code shown that filter rejection ratios ≥ 40 dB are possible. This means, that the length of superconducting RWGscan be reduced. Two RWG HOM couplers have RWGs rotated through $45^\circ - 60^\circ$. It is not possible to locate them between the 4K and 70K shields in the longitudinal direction without using of the RWG-twists.

Fig. 24 and Fig. 25 show RWGs location in the cryostat. We can see RWG loads are oriented vertically, so normalconducting parts of RWGs have a length of the order of 300 mm. Under such conditions the heat flux through the $110 \times 20 \times 0.2 \times 1000$ waveguide to 2K region increases to approximately 40 mW. It is possible to reduce this value by using of bellows-like waveguides. The last variant is very useful in both three-waveguides and two- RWG HOM couplers, because it ensures mechanical decoupling of 4K and 70K region and permits operation under different pressure inside and outside of the thin-walled RWG without any vacuum RF windows.

It is necessary to prononce the fact that the using of a rejection filter is possible only if electric and magnetic fields strength values in the filter are in acceptable limits.

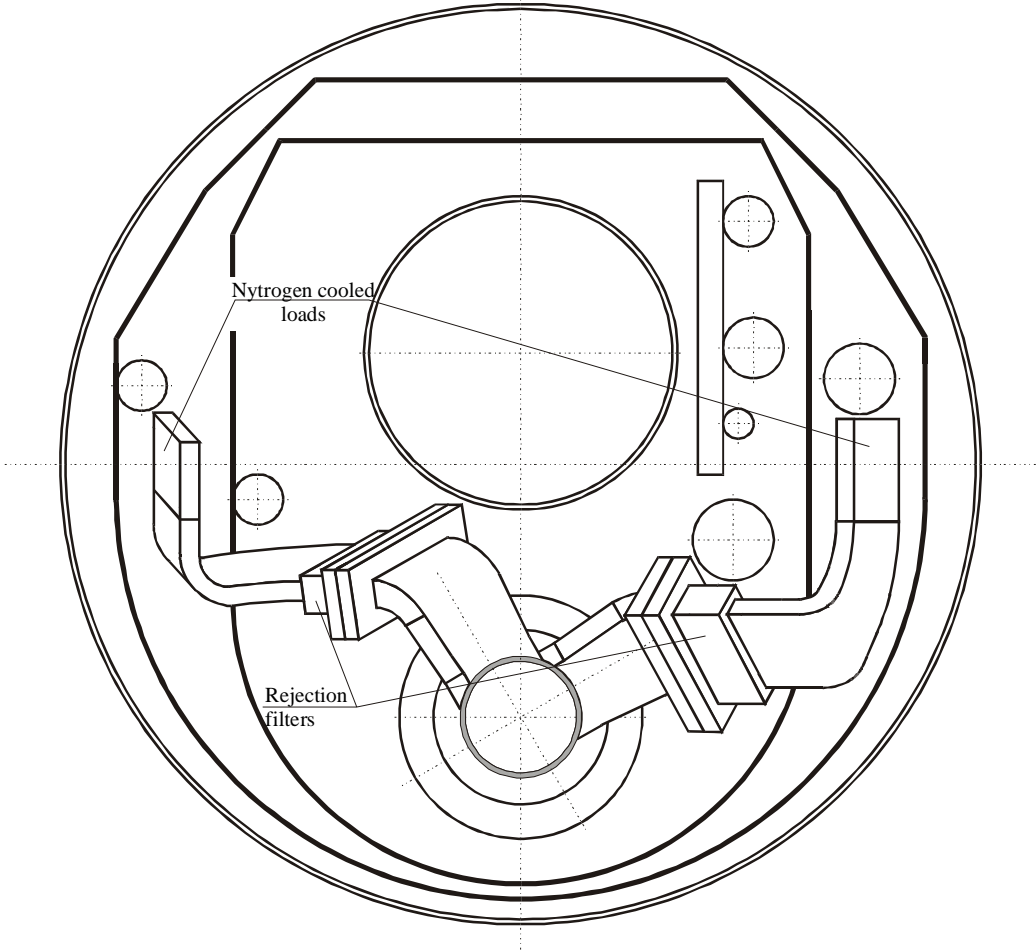


Fig.24. Two RWG HOM coupler with rejection filter. Front view

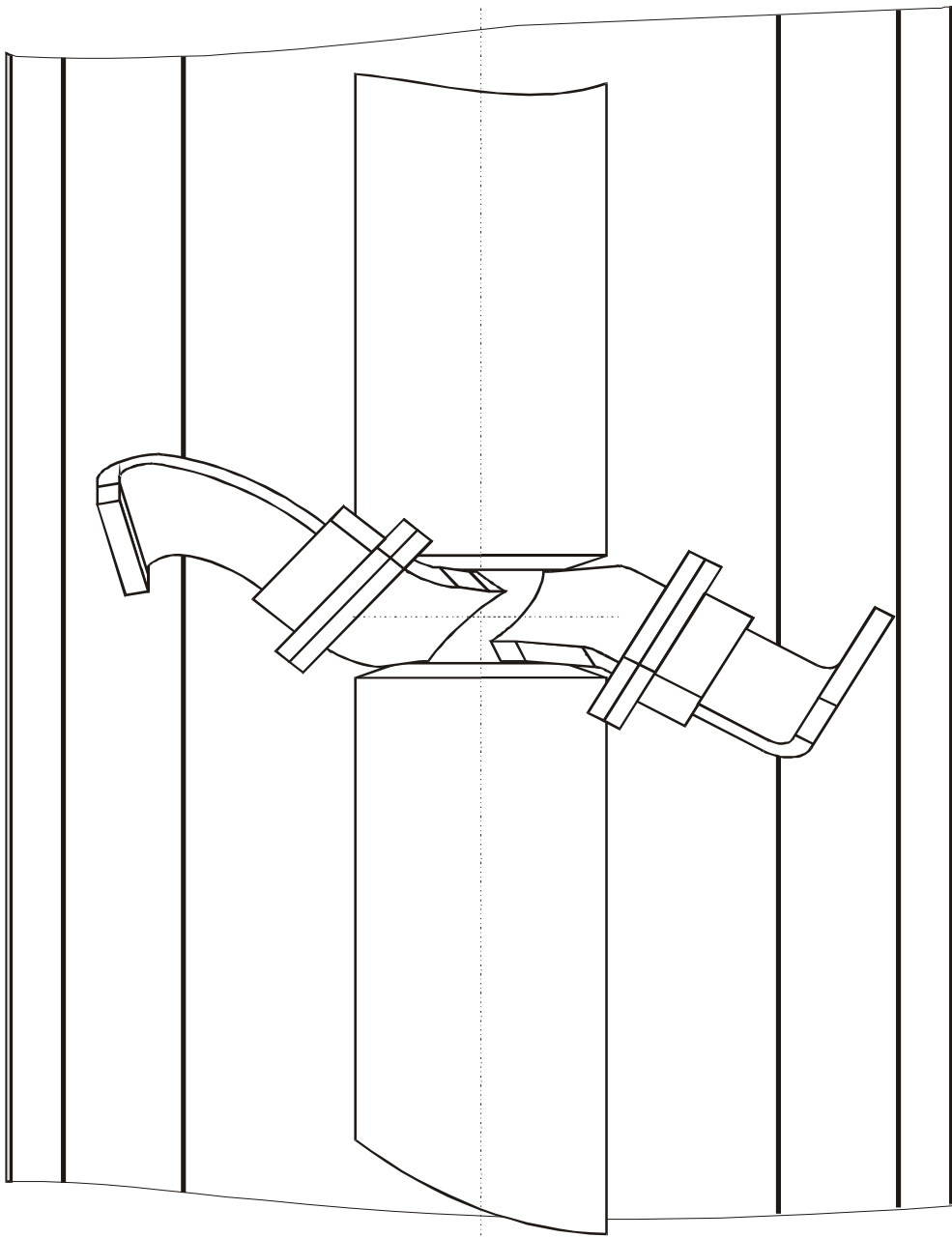


Fig.25. Two RWG HOM coupler with rejection filter. Top view

Appendix 1. Tuning of subcavities at the fundamental mode frequency.

Each subcavity was tuned at the fundamental mode frequency before brazing using the following technique. Let us f_{op} is operational frequency and f_0 is an operational mode frequency of the cavity. Field distribution along the cavity cells can be described by the following set of equations

$$\begin{aligned}
 & \left(1 - \frac{f_0^2}{f_{c1}^2}\right) E_1 - \frac{k_1}{2} E_2 = 0 \\
 & \dots\dots\dots \\
 & -\frac{k_{n-1}}{2} E_{n-1} + \left(1 - \frac{f_0^2}{f_{cn}^2}\right) E_n - \frac{k_n}{2} E_{n+1} = 0 \\
 & \dots\dots\dots \\
 & -\frac{k_{N-1}}{2} E_{N-1} + \left(1 - \frac{f_0^2}{f_{cN}^2}\right) E_N = 0
 \end{aligned} \tag{A1-1}$$

where f_{cn} is frequency of the n-th cell; $k_n/2$ is a cell to cell coupling coefficient; E_n is the electric field strength in the middle of the n-th cell; N is number of cells in the cavity.

Assuming $k_1 = k_2 = \dots = k_n = \dots = k_{N-1} = k = 0.01889$ and using experimentally measured E_n and f_0 one can calculate f_{cn} values as follows

$$\begin{aligned}
 f_{c1} &= \frac{f_0}{\sqrt{1 - \frac{k}{2} \frac{E_2}{E_1}}} \dots\dots\dots f_{cn} = \frac{f_0}{\sqrt{1 - \frac{k}{2} \left(\frac{E_{n-1}}{E_n} + \frac{E_{n+1}}{E_n} \right)}} \dots\dots\dots \\
 f_{cn} &= \frac{f_0}{\sqrt{1 - \frac{k}{2} \frac{E_{N-1}}{E_N}}} \dots\dots\dots n = 2, 3, \dots, N-1
 \end{aligned} \tag{A1-2}$$

From the other hand to provide uniform field distribution along the cavity at the operational frequency f_{op} cells frequency must satisfy the following expressions

$$f_{c1}^{op} = f_{cN}^{op} = \frac{f_{op}}{\sqrt{1 + \frac{k}{2}}} \dots\dots\dots f_{cn}^{op} = \frac{f_{op}}{\sqrt{1 + k}} \dots\dots\dots n = 2, 3, \dots, N-1 \tag{A1-3}$$

As a result we can calculate frequency detuning of the cells

$$\delta f_{cn} = f_{cn} - f_{cn}^{op} \tag{A1-4}$$

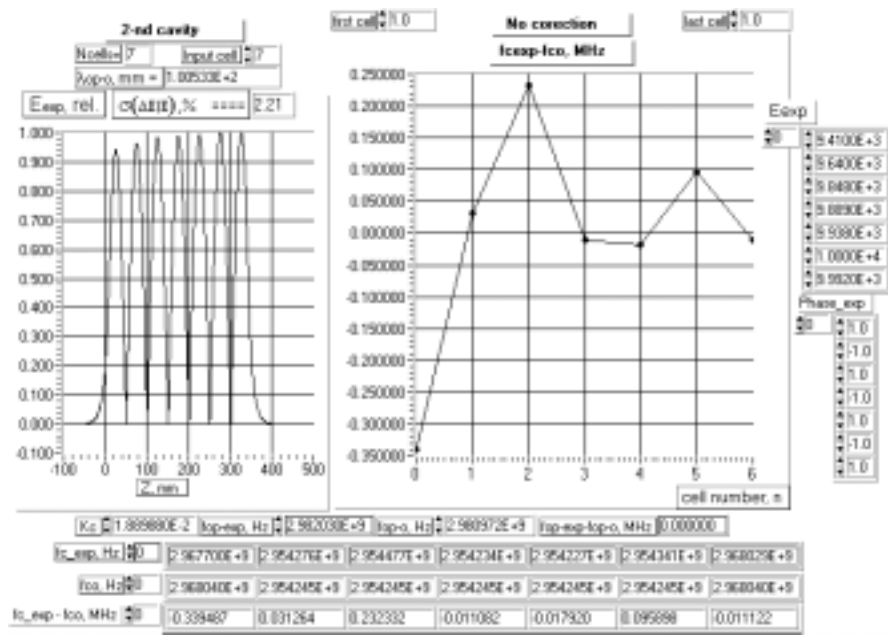
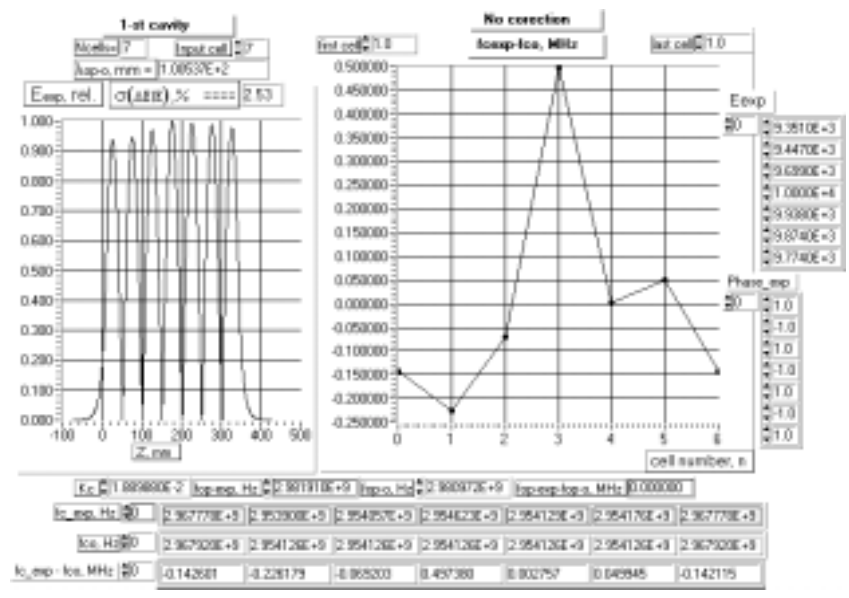
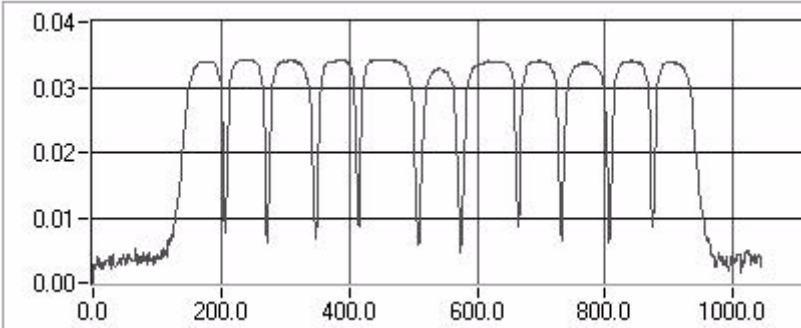
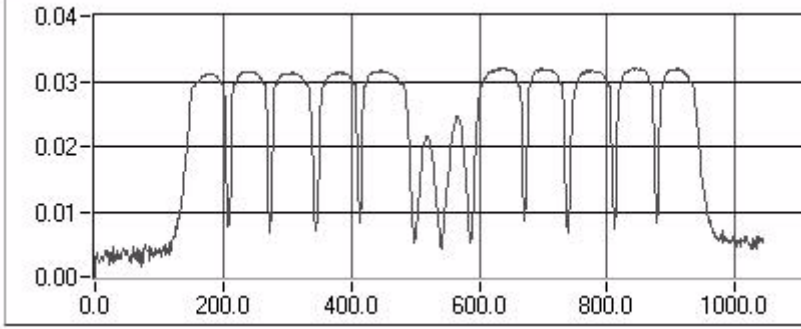
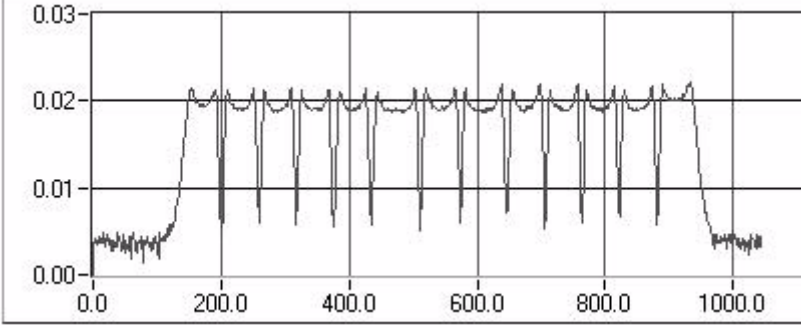
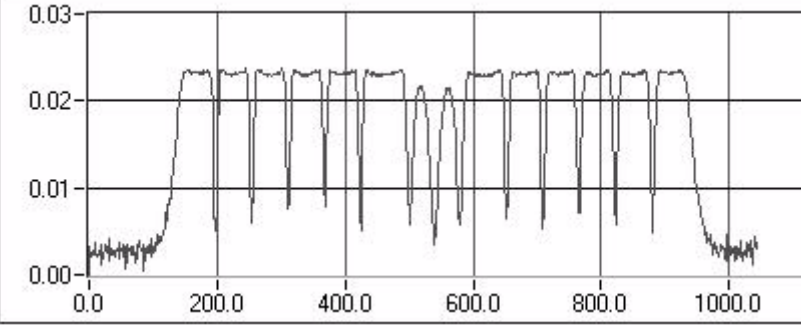
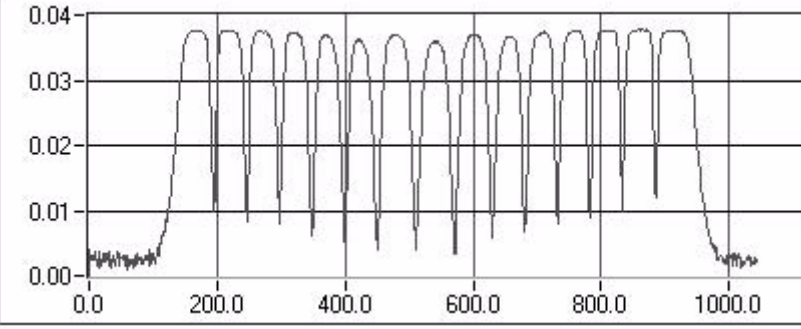
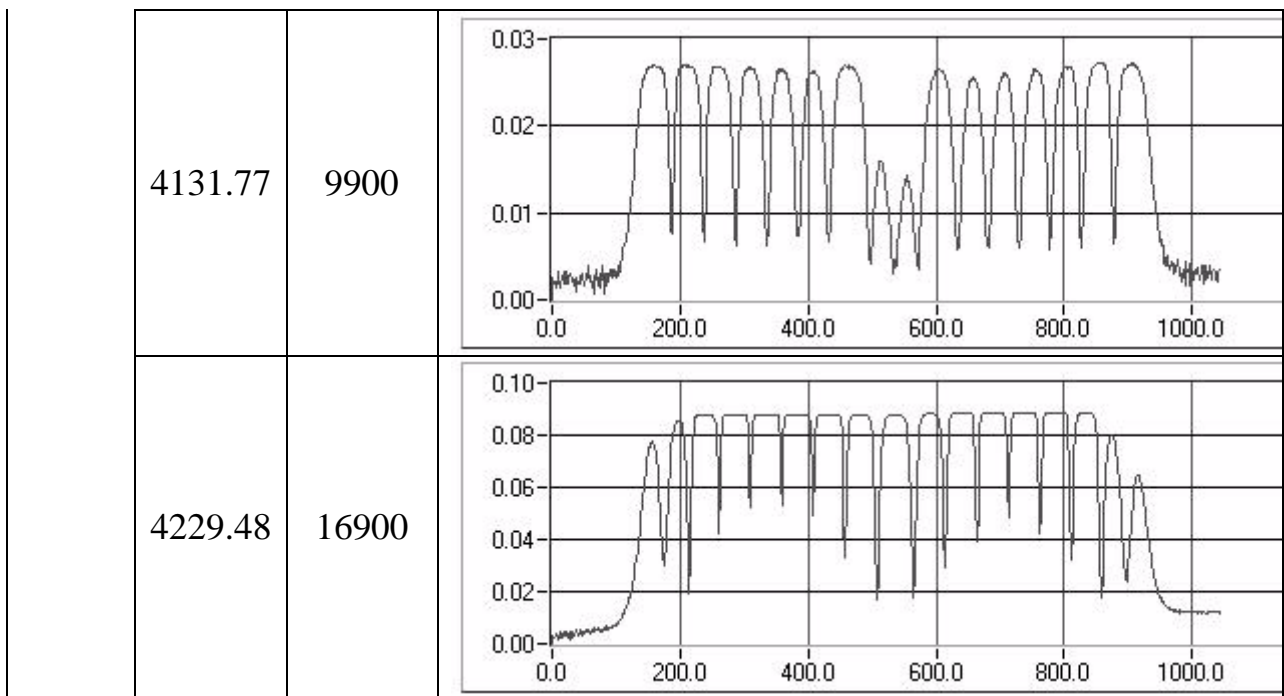


Fig. A-1. The results of smoothing of the electric field in two subcavities.

Appendix 2. Experimental data of electric field distribution at two subcavities.

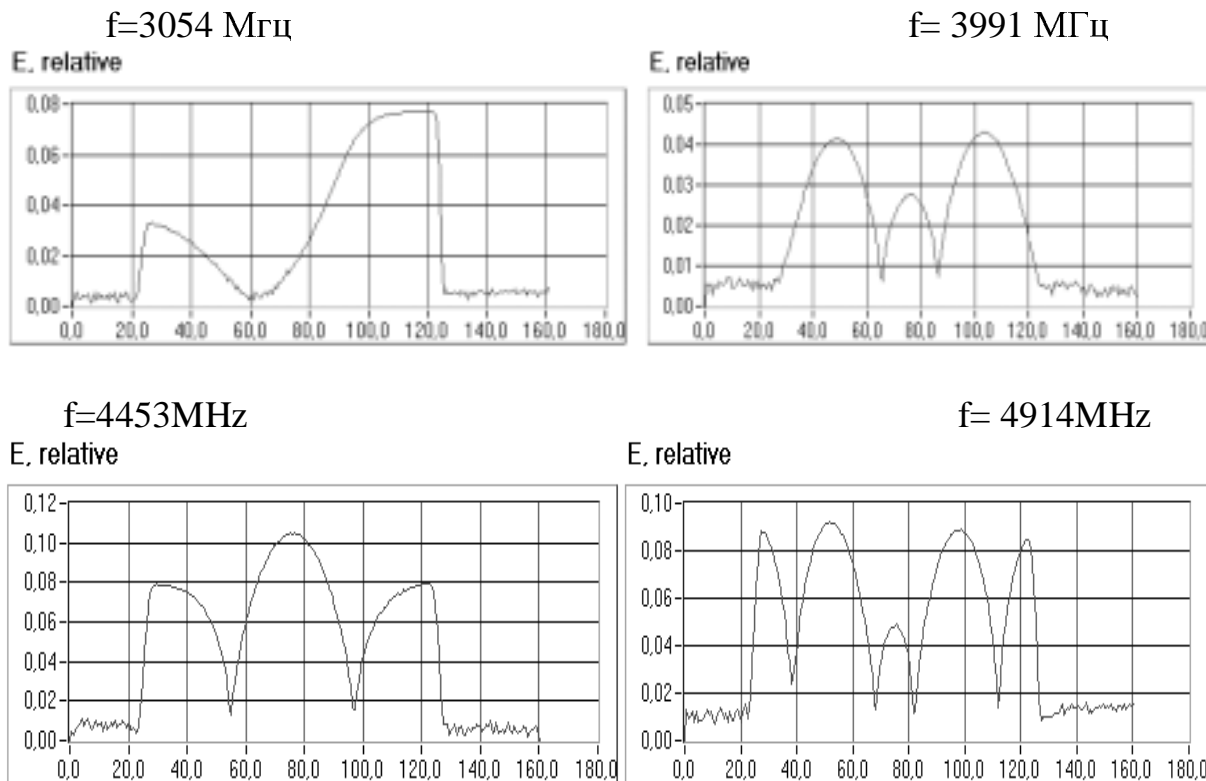
Mode	F, MHz	Q_0	
H_{111}	3744.47	9600	
	3784.07	8100	
	3840.13	12800	
	3843.10	7000	

	4000.60	10200	
	4009.21	11500	
	4074.72	10100	
	4089.85	11600	
E ₁₁₀	4127.07	10200	



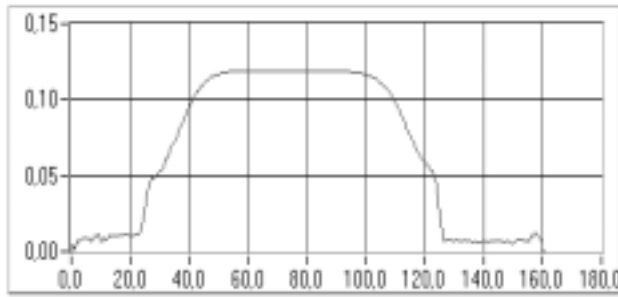
Appendix 3. Experimental data of longitudinal electric field distribution along the axis of resonance mock-up, consisting from beam pipe at $\lambda/4$ with half cells at the both ends.

Without HOM couplers.



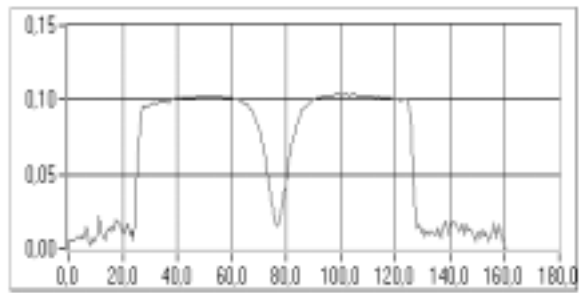
f=5005MHz

E, relative



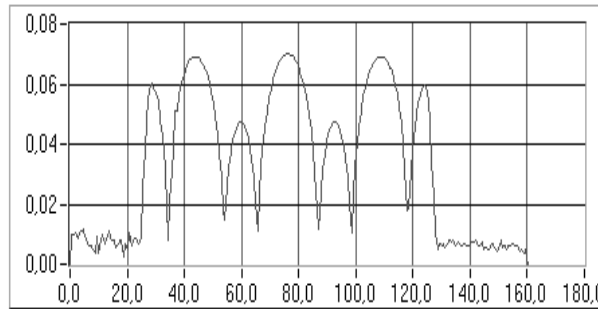
f=5719MHz

E, relative



f=5755MHz

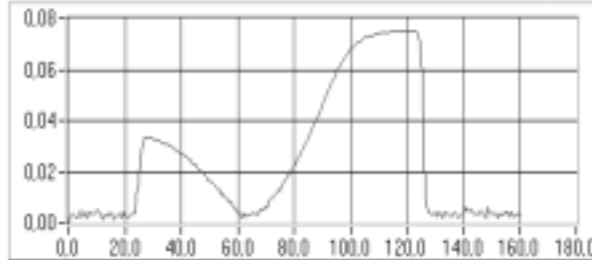
E, relative



With longitudinal disposition of HOM coupler

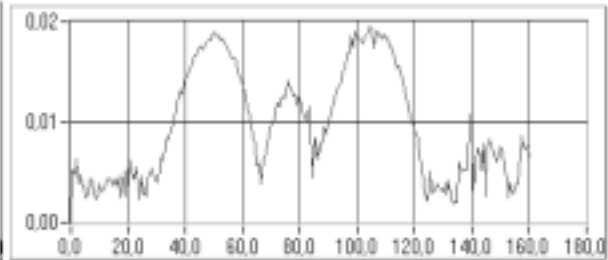
f=3055MHz

E, relative



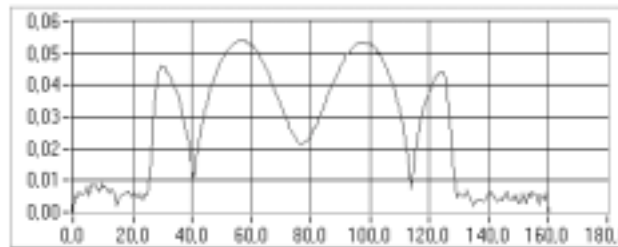
f=3976MHz

E, relative



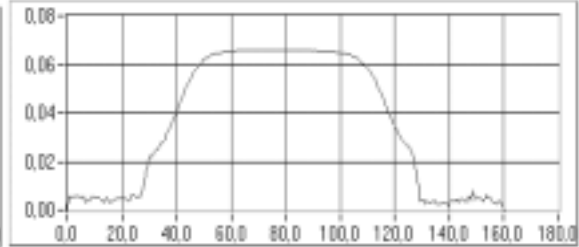
f=4880MHz

E, relative

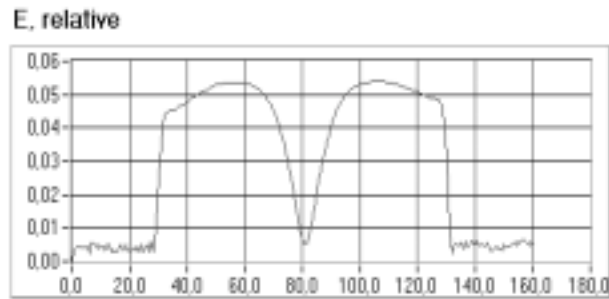


f=4955MHz

E, relative

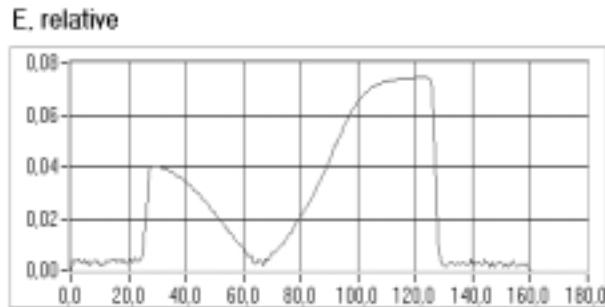


f=5703MHz

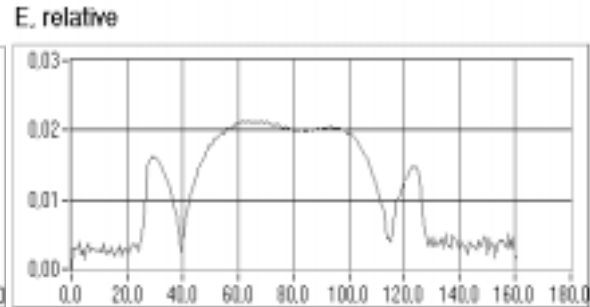


With HOM coupler at angle 60^0 to axis of beam pipe.

f=3054MHz



f= 4918MHz



f=5700MHz

References

1. Coceptual Design of a 500 GeV e^+e^- Linear Collider with Integrated X-ray Laser Facility, DESY 1997-048, ECFA 1997-182, vol.1
2. J.Boster, M.Dohlus, V.Kaljuzhny at all. Rectangular Waveguide Coupler fot two TESLA Supercavities. DESY, TESLA-99-01, 1999.
3. C.Pagani et all "Further improvements of the TESLA test facility cryostat in view of the TESLA collider" Cryogenic engineering conference, Canada, July 12-16, 1999.